Deliverable D5-WP3&10-Partner Contribution

The Use of Satellite SAR data in support of Ship Navigation in Sea Ice

the Nansen Center contributions under WP 3 and 10

Status (Restricted)

A R C D E V

Contract No: WA-97-SC.2191

Project Co-ordinator: **FORTUM OIL AND GAS (Formerly NESTE)**

West European Partners:

Kvaerner Masa-Yards Inc (KMY)
Helsinki University of Technology (HUT)
Hamburgische Schiffbau-Versuchsanstalt GmbH (HSVA)
MTW Schiffswerft GmbH (MTW)
Earth Observation Sciences Ltd. (EOS)
Tecnomare S.p.A. (Tecnomare)
Remtec Systems Ltd. (Remtec)
Shell Vankor Development B.V. (SHELL)
Lloyd's Register of Shipping (LR)
Nansen Environmental and Remote Sensing Center (NERSC)
Fachhochschule Hamburg, Institute of Ship Operation, Sea Transport and Simulation (ISSUS)

Russian Partners:

Northern Sea Route Administration (NSRA)
Central Marine Research & Design Institute Ltd. (CNIIMF)
Murmansk Shipping Company (MSCO)
Arctic Shipping Services (ASS)
Krylov Shipbuilding Research Institute (KSRI)
State Research Center of Russian Federation - Arctic and Antarctic Research Institute (AARI)

Date: **June 1., 1999**

PROJECT FUNDED BY THE EUROPEAN COMMISSION UNDER THE TRANSPORT RTD PROGRAMME OF THE 4TH FRAMEWORK PROGRAMME

The Nansen Environmental and Remote Sensing Center

a non-profit
research institute affiliated with
the University of Bergen

Edv. Griegsvei 3a,
N-5037 Solheimsviken
Norway

NERSC Technical Report no. 167

Arctic Demonstration and Exploratory Voyage (ARCDEV)

THE NANSEN CENTER CONTRIBUTION TO
WP3: ICE CONDITIONS
AND
WP10: REMOTE SERVICES AND MAINTENANCE

Under contract with
Commission of the European Communities
DG7 – Transport RTD Programme
Contract no: WA-97-SC.2191

by
Lasse H. Pettersson, Stein Sandven, Øyvind Dalen,
Vladimir V. Melentyev, Andrey Bogdanov,
Kjell Kloster, and **Maria Lundhaug**

Bergen, June 1, 1999

Nansen Environmental and Remote Sensing Center
Edv. Griegsvei 3a
N-5059 BERGEN
NORWAY
Phone: +47 55 29 72 88 Fax: +47 55 20 00 50
e-mail: lasse.pettersson@nrsc.no
URL: http://www.nrsc.no

NERSC

a non-profit environmental research center
affiliated with the University of Bergen

REPORT

TITLE Arctic Demonstration and Exploratory Voyage (ARCDEV) NERSC contribution to WP3: Ice conditions and WP10: Remote Services and maintenance	**REPORT No.** Technical report no. 167
CLIENT CEC – DG VII Transport RTD Programme	**CONTRACT No.** WA-97-SC.2191
CONTACT PERSON José Anselmo, CEC DG VII **PROJECT COORDINATOR**: Ivan Ivanov, Fortum Oil & Gas OYJ	**AVAILABILITY** Open
AUTHORS Lasse H. Pettersson, Stein Sandven, Øyvind Dalen, Kjell Kloster, and Maria Lundhaug (NERSC) Vladimir Melentyev and Andrey Bogdanov (NIERSC)	**DATE** June 1, 1999
ARCDEV PROJECT PARTNERS: Fortum Oil and Gas OYJ, FI; Earth Observation Sciences Ltd, UK; Helsinki University of Technology, Ship Laboratory, FI; Hamburg Ship Model Basin Ltd, DE; Institute of Ship Operations, Sea Transport and Simulation, DE; Kvaerner Masa Yards, FI; Lloyd's Register of Shipping, GB; Aker - MTW Shipyard, DE; Nansen Environmental and Remote Sensing Center, NO; Remtec Systems Ltd, FI; Tecnomare S.p.A., IT; Shell Vankor Development, NL; The Russian Federation Ministry of Transport, RU; Administration of the Northern Sea Route, RU; Arctic and Antarctic Research Institute, RU; Arctic Shipping Services, RU; Central Marine Research and Design Institute, RU; Krylov Ship Research Institute, RU; Murmansk Shipping Company, RU	
APPROVAL Lasse H. Pettersson	 Ola M. Johannessen, Director

1 INTRODUCTION

The Kara Sea and the Yamal Peninsula are among the largest oil and gas reservoirs of the Russia Federation Production. Active production is now carried out at Bovanenkovo, Cape Kharasavey, Tambey, Sabeta and others. Also several new oil and gas reservoirs are identified. Experts evaluate the gas resources around the Ob-Yenisey estuaries to be more than 15 trillion m^3. Throughout the year ice in the Kara Sea create problems for oil and gas production in the shelf regions, especially for routing operations of tankers and cargo ships during the ice season.

The objective of the Arctic Demonstration and Exploratory Voyage (ARCDEV) project was to investigate the constraints of year-round ship transportation of gas condensate from the Ob river in the western Siberia, by using the Finnish "ice class" tanker M/T Uikku. The exploratory voyage lasted from April 26 to May 15 1998. M/T Uikku represents a new type of tankers, build for operations in sea ice, and has operated in the Arctic region for several years. In order to perform scientific investigations during the expedition the i/b Kapitan Dranitsyn hosted about 80 scientists performing auxiliary investigations. The nuclear icebreakers Rossia and Vaygach from Murmansk Shipping Company (MSC) supported the convoy through parts of the journey, i.e. through heavy pack ice in the Kara Sea, and by preparing a channel through the fast ice in the Ob estuary. The scientific programme included extensive sea ice investigation and observations, in addition to ship performance studies.

The Nansen Center participated under WP3 - *Ice conditions* - where the main objectives were to create basic information on the ice conditions for the convoy and scientific studies, and to demonstrate practical use of satellite microwave radar data to map the ice conditions in support of navigation. The responsibility of the Nansen Center was to provide near real time access to satellite SAR data of the alternate sailing route in the Barents, Pechora and Kara seas (including the Ob estuary), as support for ship operation planning, ice navigation and detailed mapping of the ice conditions along the route.

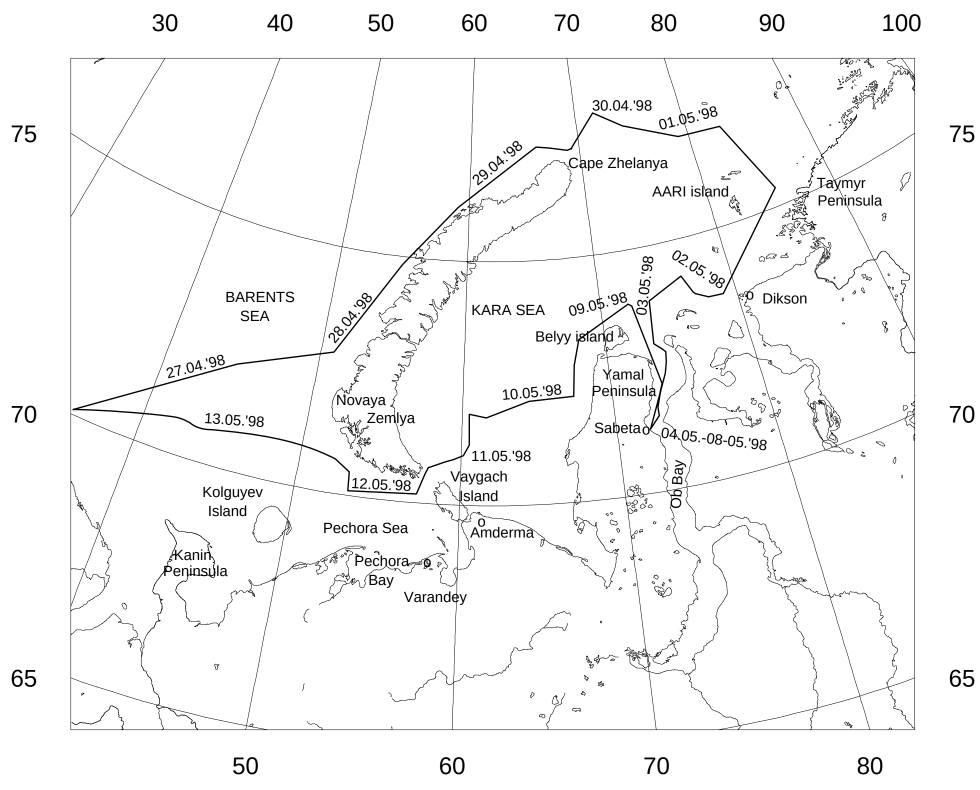

Figure 1. The expedition route from day to day. The map also shows the geographical position for the place names used throughout the report.

Of particular interest with the ARCDEV expedition is that this was the first winter ice navigation operation in the Ob estuary. Demonstration of the possibility for year-round navigation in this estuary is extremely important for the entire oil and gas industry. The expedition included both practical use of satellite radar technology as support for ship navigation as well as collection of extensive sea ice information for validation of the satellite data.

2 PRACTICAL USE OF SAR FOR ICE NAVIGATION SUPPORT

Synthetic Aperture Radar (SAR) sensors have been regularly available from satellite platforms since the launch of the European ERS-1 satellite in 1991, and used in the Russian Arctic since 1993. Currently ERS-2 and the Canadian satellite RADARSAT provide SAR information used for support in ship navigation in ice covered areas [Johannessen *et. al*, 1994, Sandven 1998b]. The swath width of the two instruments is respectively 100km and 500km (ScanSAR). The two radar systems have different polarisation and incidence angle, which impact on analyses of images from the two satellites. Being an active instrument, the SAR sensor is independent of day light and weather conditions (i.e. hazard, haze and clouds). Further, the radar signals penetrate dry snow completely and to some extent also the surface of ice. Thus making it an efficient instrument for measuring the Arctic ice cover. Use of ERS-1/2 for ice navigation support has become a routine operation. Practically all icebreaker crew are educated and have large experience with operational application of SAR data for selecting optimal route in the ice. Major Russian icebreakers are now equipped with adequate hardware and software for utilising this kind of information. SAR images files can be received digitally onboard the icebreaker using a modem and the INMARSAT telecom satellite system [e.g. Johannessen *et. al*, *1999*].

The main sea ice parameters retrievable from SAR data are the ice development (age), the form and shape of both drift and fast ice, ice concentration (including partial concentration), ice movement processes, ice arrangements, openings in the ice (cracks, leads and fractures), surface characteristics including rafting and ridging, and open water surface characteristics, including wind speed.

Characteristic RADARSAT ScanSAR signatures of different ice types have been retrieved on the basis of sub-satellite visual ice observation and classification, photographs, and joint analysis with ERS SAR data. The RADARSAT signatures of new and young ice varies considerably, depending on the ice type and actual state of the surface. Nilas is seen as homogenous areas with low backscatter values, while grey ice have a very high signal, and is clearly distinguishable from nilas. The brightness of grey/white ice varies from dark to rather light, depending on thickness and surface deformation. First-year ice will vary from dark to light, mainly depending on the degree of ridging. Level ice give a very dark backscatter signal, while heavy ridged and deformed first-year ice can be as bright as grey ice. Although the image brightness values of first-year ice and grey or grey/white ice tend to be similar, they can be separated due to differences in the texture. Level land-fast first-year ice has a very dark signature value, very similar to calm open water. Contextual information, such as position and time of the year, is often necessarily in order to separate these two situations. Leads and fractures, both unfrozen or covered with new or young ice, can be identified in RADARSAT images. This information is very important for selecting an optimal navigation route in the ice.

2.1 SATELLITE DATA ACQUISITION AND TRANSMISSION TO ICEBREAKER

WP10: Remote Services and Maintenance involved procedures to make satellite radar data available onboard the ARCDEV vessels. Satellite radar images from the ESA ERS-1 and Canadian RADARSAT SAR sensors were downloaded and processed at Tromsø Satellitt

Stasjon (TSS), which required 1-2 hours delay time to process near real-time SAR data. A version of the image sufficient for ice decoding is then transferred via FTP to a server at NERSC. If requested, a full resolution version of the image is later available on CDROM for mail distribution. At NERSC a backscatter normalisation is performed in order to preserve an approximately homogenous intensity across the image in range direction. Thereafter, the image is geo-rectified using satellite acquired corner-positions, contrast enhanced, and superimposed shorelines and a geodetic grid as the baseline for the interpretation. Data reduction using JPEG compression produces an image file of about 200kB. The work done at NERSC takes about one hour. Using modem and transmission via INMARSAT the images can be collected in digital form by personnel onboard the icebreaker. The file transmission takes approximately 10-15 minutes. Unfavourable local conditions can cause trouble for the transmission at latitudes at the edge of the INMARSAT coverage. Between three and four hours after acquisition the image is onboard for analysis of ice conditions and ship routing. The data flow from image acquisition to onboard distribution is shown in Figure 4.

A total of 15 RADARSAT ScanSAR and ERS-2 SAR images were received in near real time onboard i/b Kapitan Dranitsyn during the expedition time (Figure 2 and Figure 3). A brief description of each image is shown in Table 1. Additionally 13 RADARSAT and ERS-2 SAR images were acquired before the expedition started, and used in the same manner. Especially valuable of the later images, were two ERS-2 scenes of April 17, which covered the fast ice zone in the Ob estuary. This mosaic was used for a detailed planning of a channel in the fast ice, later prepared by ni/b Vaygach.

2.2 SAR DATA ACQUISITION DURING ARCDEV

During ARCDEV the SAR data were used as support for practical ice navigation and loading operations. Extensive experience of analysing ERS SAR ice data, and *in situ* data obtained along the route helped in the analysis and interpretation process.

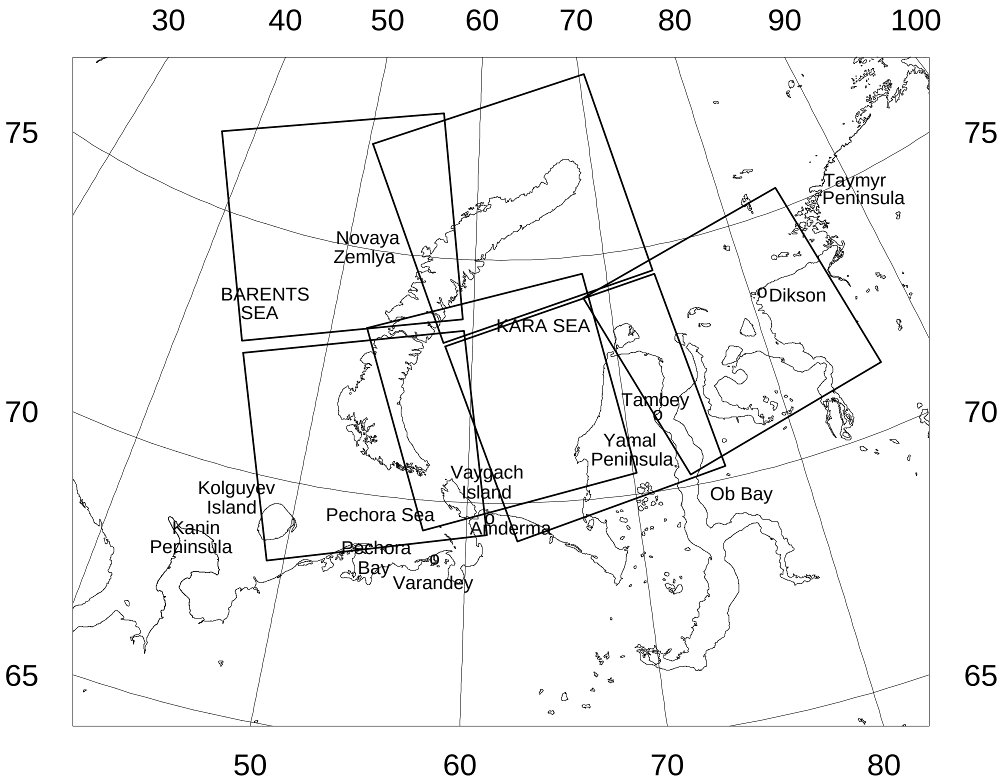

Figure 2. Coverage of RADARSAT ScanSAR scenes from April 23 to May 8, 1998.

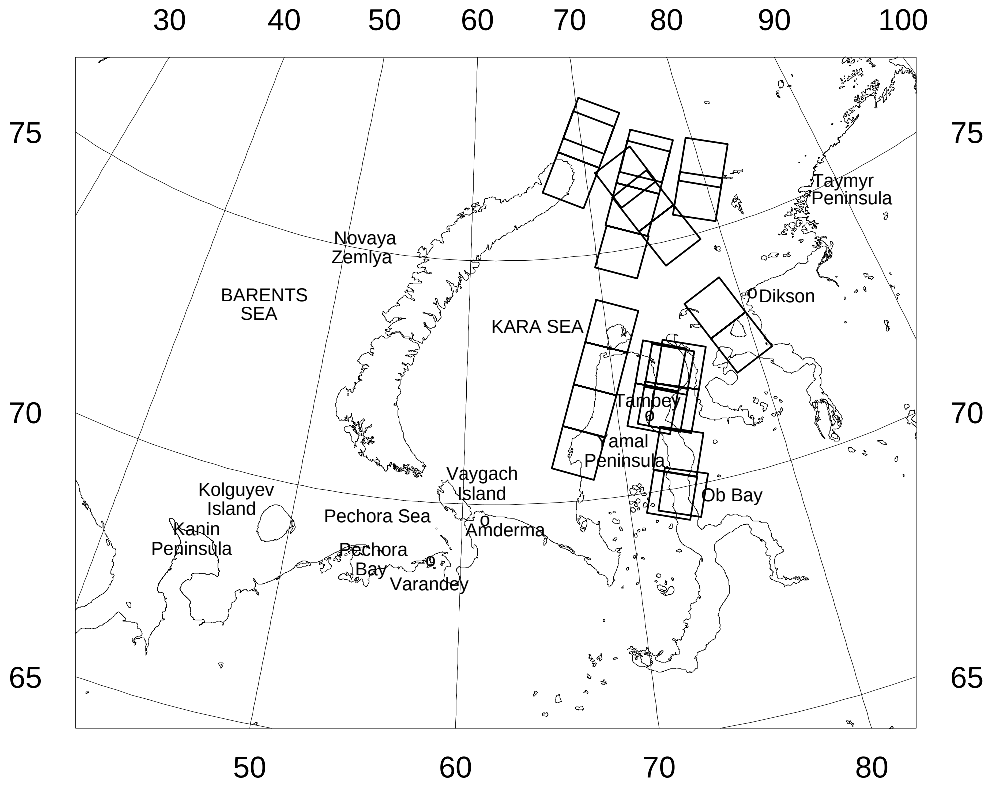

Figure 3. Coverage of ERS-2 SAR scenes from April 10 to May 6, 1998.

The tasks of using SAR data included

1. using historical SAR data for strategic planning of ice navigation operations
2. ordering new data acquisitions covering the areas of potential routes
3. near real-time distribution of SAR data to the icebreaker Kapitan Dranitsyn and its crew
4. analysis and interpretation of the data onboard

using the SAR data as support in both strategic and tactical navigation planning, for selecting the optimal route in the ice (both drift ice and fast ice)

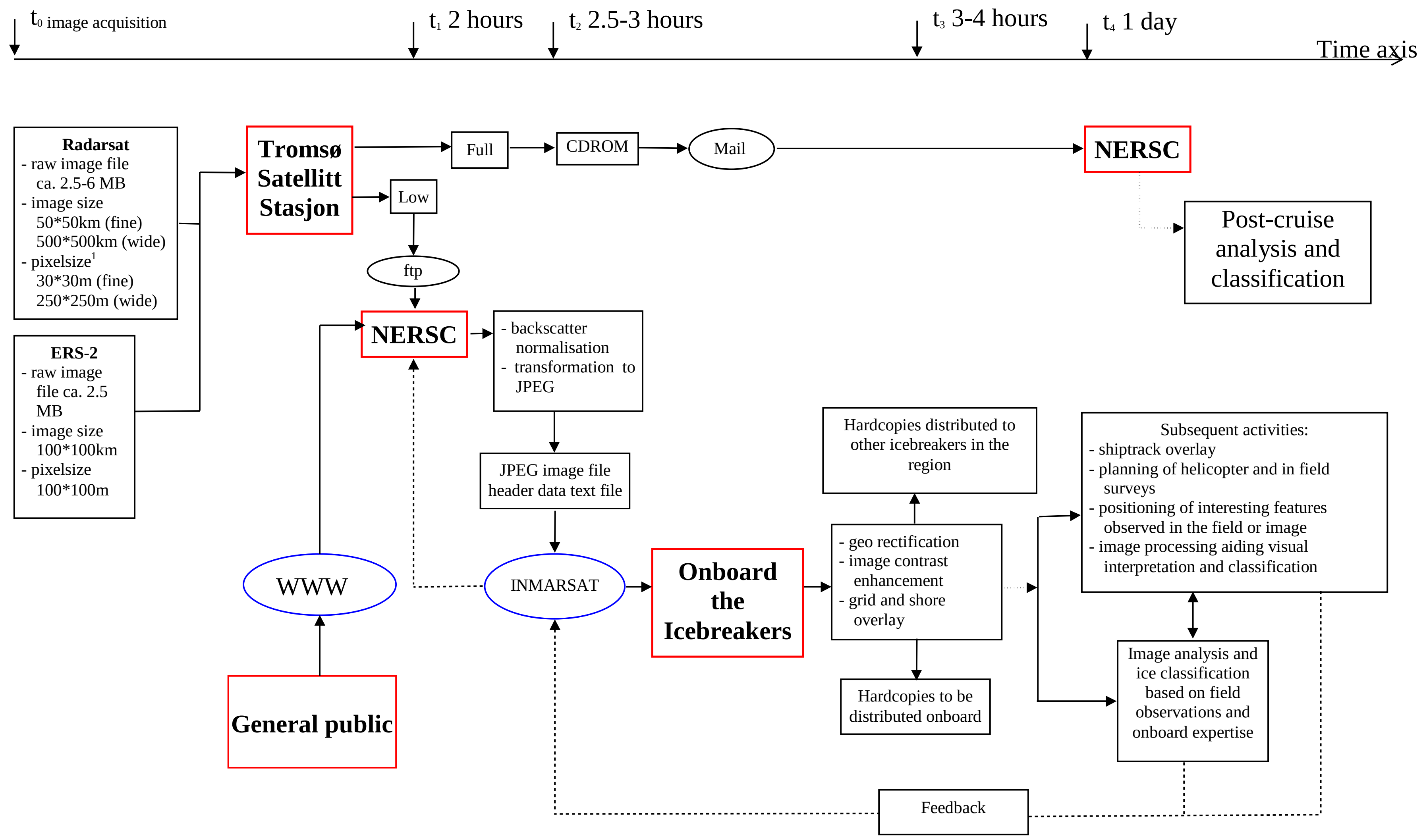

Figure 4. Data float scheme for the SAR images acquired during the ARCDEV expedition.

Satellite	Area covered	Acquired (GMT)	Ship position when acquired	Received (GMT)	Comments on time of data arrival onboard i/b Kapitan Dranitsyn and use
ERS2 (2 images)	71°15'N/71°E 73°N/75°E	17.04 06:45	-	17.04	Received prior to voyage, used for planning of i/b Vaygach's preparation of a channel in the Ob gulf.
RADARSAT SW	73°N/40°E 77°N/55°E	23.04 13:45	In Murmansk	23.04 17:00	Prior to arriving in the image area, used by MOH for planning of route from the ice edge towards the polynya NW of Novaya Zemlya.
RADARSAT SW	69°N/46°E 73°N/60°E	23.04 13:45	In Murmansk	30.04 19:30[1]	Not covering our route towards Ob, but used by MOH for planning of route for i/b Sovietskiy Soyuz and Rossia, and for planning of our return voyage.
RADARSAT SW	74°N/55°E 78°N/70°E	25.04 12:44	In Murmansk	26.04 12:00	Prior to arriving in the image, displays the grey and grey/white ice in the polynya NW of Novaya Zemlya.
RADARSAT SW	70°N/60°E 74°N/74°E	25.04 12:44	In Murmansk	30.04 19:30[1]	Not covering our route towards Ob, but used by MOH for planning of route for i/b Sovietskiy Soyuz and Rossia, and for planning of our return voyage. Together with RADARSAT of 08.05.1998 used to estimate the general ice drift along the western shores of Yamal Peninsula. Used by MOH for planning of route for another convoy operating in the Kara Sea, with direction towards the western shores of Yamal Peninsula, and together with ERS2 of 10.04 used for planning of this convoy's operation in the fast ice zone towards a temporally oil loading station close to Kharasavey.
ERS2 (2 images)	76°N/66°E 77.5°N/73°E	25.04 07:35	In Murmansk	26.04 09:00	Prior to arriving in the image area, the polynya shown was closed when the convoy arrived.
ERS2 (3 images)	74.5°N/70°E 77°N/77.5°E	29.04 07:09	77°19'N/ 66°02'E	29.04 19:30	Not covering our route towards Ob, due the late change of route north-eastwards from Novaya Zemlya.
RADARSAT SW	71°N/70°E 75°N/85°E	30.04 11:58	77°13.6'N/ 69°17.4'E	30.04 19:30	Prior to arriving in the image area, used by MOH for planning of the route from Taymyr Peninsula towards, and into the Ob Gulf.
ERS2	69.5°N/71.5°E 70.5°N/75°E	30.04 06:39	77°13.6'N/ 69°17.4'E	30.04 19:30	Not covering the route, south of Tambey/Sabeta.
ERS2 (2 images)	71°15'N/72°30'E 73°N/76°30'E	03.05 06:45	73°53.2'N/ 73°37.3'E	03.05 19:30	Prior to arriving in the image area, used for validation of the prepared ice channel.
ERS2 (2 images)	71°15'N/71°E 73°N/75°E	06.05 06:45	71°18.1'N/ 72°08.7'E (Sabeta)	06.05 19:30	Describes the channel after our convoy passed, used to evaluate the state of the channel before our return voyage.
RADARSAT SW	70°N/54°E 74°N/70°E	08.05 13:05	72°03'N/ 73°14'E	08.05 17:00	Prior to arriving in the image area, used by MOH for planning of our route across the Kara Sea, through the Kara Gate, and into the Pechora Sea.

[1]Due to a misunderstanding regarding the route, these 2 images was cancelled, and then after request, re-ordered a few days after acquisition.

Table 1. Acquisition of SAR images for the ARCDEV expedition.

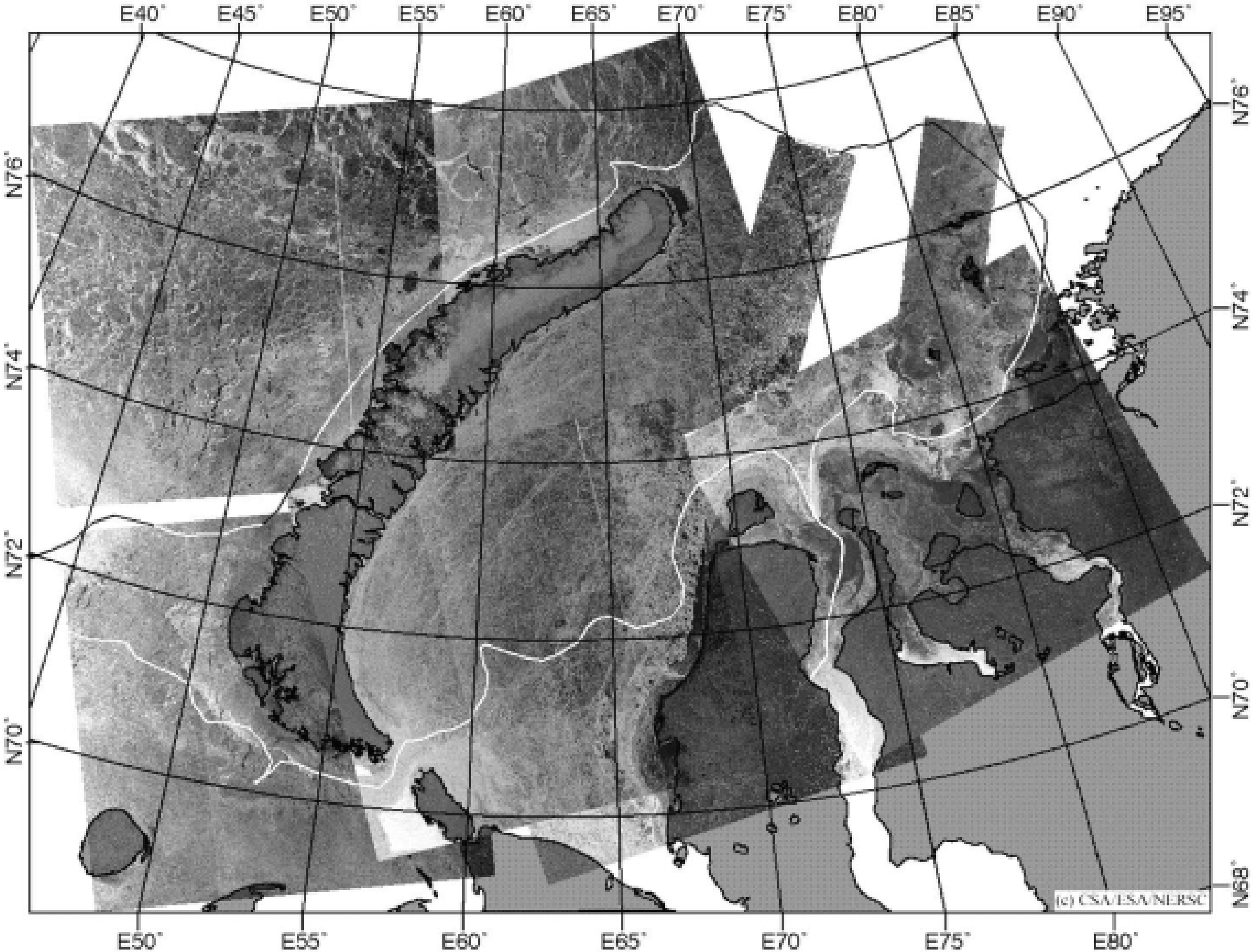

Figure 5. A mosaic of all the RADARSAT ScanSAR and ERS-2 SAR scenes acquired for the ARCDEV expedition.

3 ICE CONDITIONS ALONG THE SAILING ROUTE

Analysis of weather observations from different parts of Russian Arctic during the 1997-1998 winter season, conclude that this specific winter can be termed from severe to very severe. At the end of April practically the entire Kara, Pechora and White seas were covered with ice. In the second half of April and the beginning of May the Western Arctic was dominated by eastern winds, producing difficult ice conditions at the Kara Gate region and the surrounding waters. The eastern and western entrances to the Kara Gate and Yugor Straits were practically blocked. The result was major ice navigation difficulties in the Pechora Sea, with especially hostile conditions in the Southwestern part of the Kara Sea. A further consequence of the wind situation was a long-time pressure on the ice cover, and heavy prolongation of ridging processes.

Prior to the voyage a total of 13 RADARSAT ScanSAR and ERS-2 SAR scenes were acquired, analysed and used in the strategic planning of the route. Further, a total of 6 RADARSAT ScanSAR and 9 ERS-2 SAR scenes were acquired during the expedition time, and analysed together with MOH (N. Babich). All SAR data were acquired and received onboard before to the icebreaker entered the monitored area. Due an unexpected 2-days delay of the voyage’s departure from Murmansk, a few of the SAR scenes were acquired somewhat too early to be useful in the tactical navigation planning. Nevertheless, the images gave a relevant overview of the general ice situation, and were important in the strategic routing planning.

In total, the SAR scenes covered some $1.3*10^6 km^2$. In other words, practically the whole Kara Sea and most of the alternate sailing route, i.e. all alternatives for southern and northern variants of traditional wintertime navigation routes between the Barents and the Kara Sea.

Of special importance of the pre-voyage images, was 2 ERS-2 SAR scenes of April 17, covering major parts of the Ob estuary. This dataset was used for planning of a navigation channel through the fast ice inside the estuary. Based on the interpretation of the image, a list with geographical co-ordinates for the recommended route was send to the ni/b Vaygach. As result, the first ever winter ice navigation operation in the Ob estuary was a success. The channel was later used by the ARCDEV convoy on April 3-4 and May 8-9.

3.1 RADARSAT SCANSAR OF APRIL 23, 13:43 GMT

The most commonly used sailing route between the Barents and the Kara Sea is through the Kara Gate. The RADARSAT ScanSAR image of April 23 (13:43 GMT) resolves the ice conditions at the Kara Gate and its surrounding waters. The ice edge was located just north-west of the upper left corner of the image. From analysis of the image, it can be concluded that the ice conditions at the Pechora and Kara seas are very heavy. The Kara Sea is covered by consolidated thick and medium weathered first year ice. The crammed and hummocked first year ice creates a particular difficult navigation situation. The form of the drifting ice varies, with a predominately floe size of 0.5 – 2km. At the Kara gate region the floesizes are about 100 – 500m. The ice concentration in the northeastern part of the Pechora Sea and the part of the Kara Sea covered in the image is 10/10.

A change of direction of the local winds from northwest and west at April 22 to southeast on April 23 initiates new ridging processes, as can be retrieved in the SAR image. As result, the Novozemelsky ice massif stopped its southward displacement, and a narrow shore polynya along the eastern coast of Novaya Zemlya begins to close. Several large consolidated ridges are formed, which gives a bright radar signal. The general orientation of these new ridges is east-westwards, while older ridges are orientated from southwest to north-northeast. Hummocked and ridged thick and medium consolidated first year ice dominate (partial concentration - 7-8) west of Vaygach Island, which creates navigation difficulties at the western entrances to the Kara Gate and to the Yugor Strait. The Yugor Strait is covered by thick level fast ice. Similar fast ice conditions can be found at the southern and southwestern shores of the Novaya Zemlya archipelago.

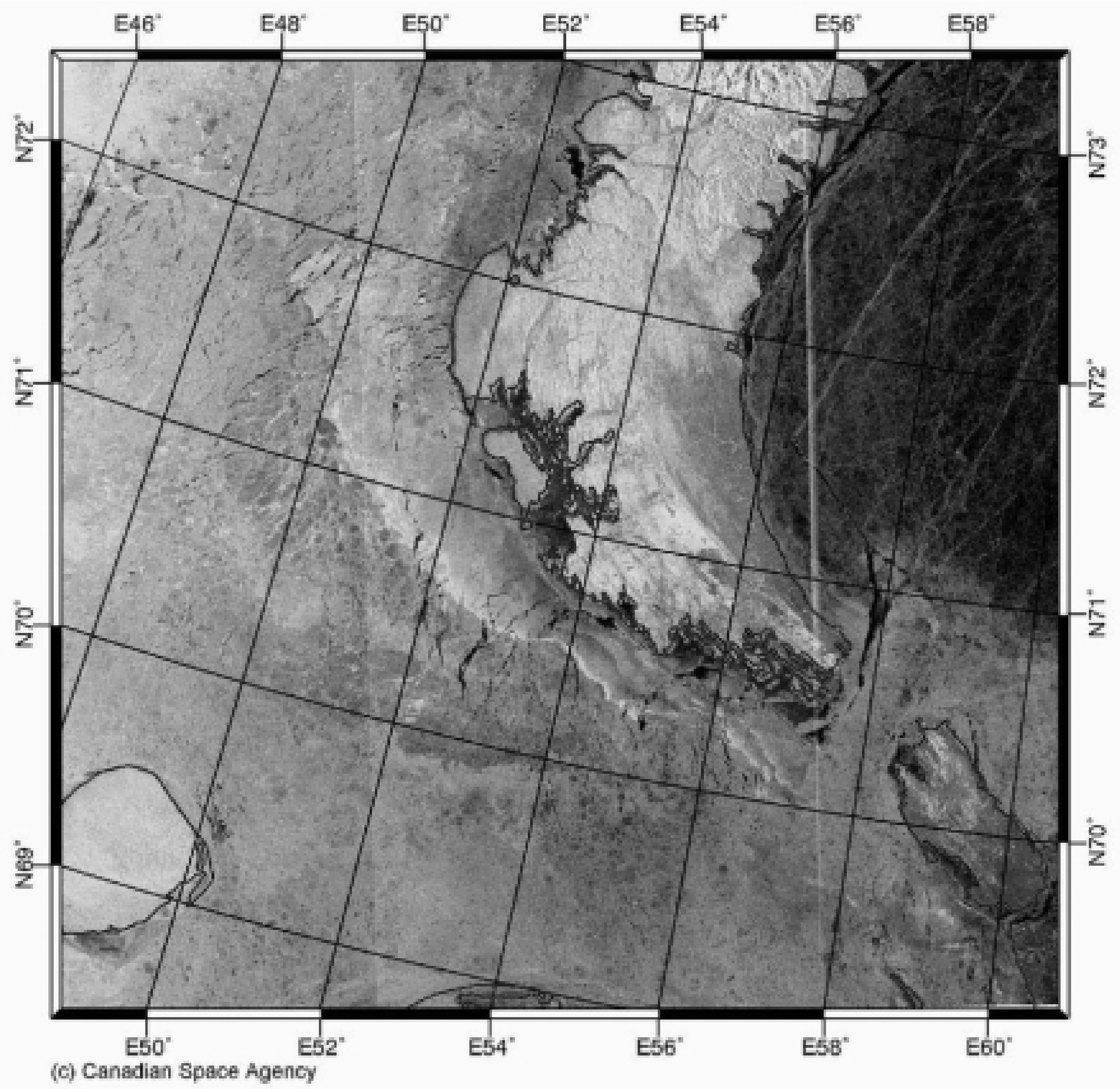

Figure 6. RADARSAT ScanSAR of April 23, 13:43 GMT, covering the Kara Gate region.

The ice conditions near Kolguev Island are less complex. Here the ice cover is thinner and varies from open to close pack ice. The before mentioned change of the wind direction initiates openings of new fractures in the Pechora Sea, and a northward displacement of the Pechorsky ice massif.

The ice cover at the coastal zones of Novaya Zemlya is thinner, dominated mainly by grey and grey/white ice. As a consequence large-scale rafting processes started at the Pechora and Barents seas southwestwards from Novaya Zemlya. New fractures are assumed to be either ice free or covered by grease ice, as both features produce a dark brightness signature.

The general conclusion of the analysis is that the ice conditions in the Pechora Sea and the southwestern part of the Kara Sea is hostile, while the ice condition along the western shores of Novaya Zemlya are more preferable for ice navigation. The i/b Kapitan Dranitsyn was not inside the area covered on its way to the Ob estuary.

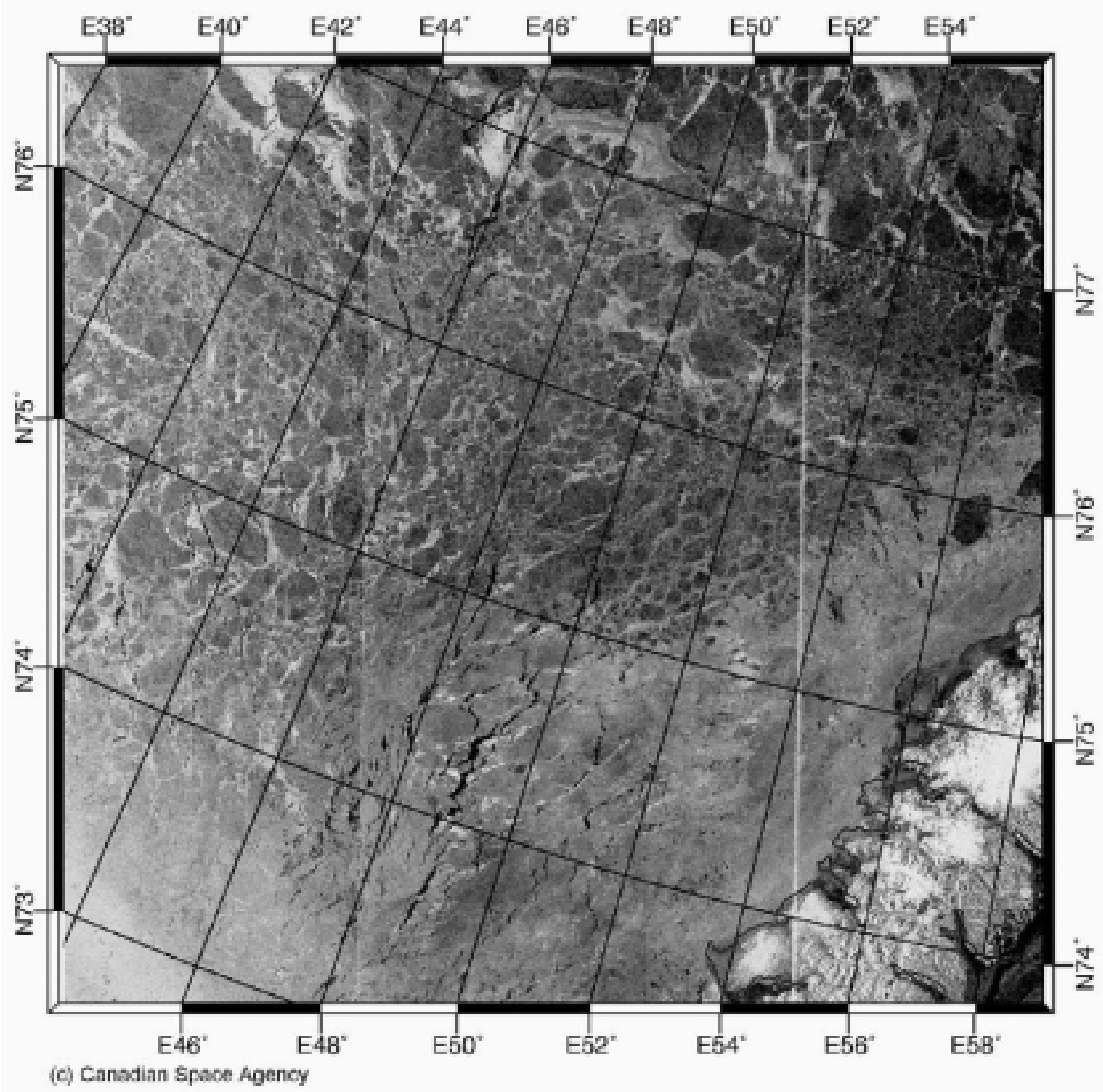

Figure 7. RADARSAT ScanSAR of April 23, 13:44 GMT, covering the Barents Sea west-northwest of Novaya Zemlya.

3.2 RADARSAT SCANSAR OF APRIL 23 13:44 GMT

The strategic planning of the ARCDEV convoy operations needed information about ice conditions at the western and northwestern coast of Novaya Zemlya, which was possible with the RADARSAT ScanSAR image of April 23 (13:44 GMT). This alternative sailing route is seldom used in the winter season, and such satellite coverage was initially not planned for the ARCDEV expedition. The analysis show that the northern and northeastern part of the Barents Sea was dominated by weathered thick and medium first year ice. Old fractures are covered by grey (including pancake) and grey-white ice. The image allows for suggestion of several routing alternatives with lighter ice conditions. Further, the image shows a well-developed polynya outside the western shore of Novaya Zemlya. This recurring polynya was covered mainly by grey and grey/white ice.

Several separate fast ice zones can be seen close to the Novaya Zemlya shores. A channel with broken ice in the shiptrack of ni/b Sovetskiy Soyuz can be seen as a thin bright line in a southeast-northwestern direction in the image. The channel can be used for dividing the stage of young ice development (age) in this area. The ice in which the channel can be seen consists of grey/white ice. Farther south in the polynya the channel disappears, and as such the ice type is grey ice (thinner).

Two large weathered thick first year ice floes, that should be avoided when sailing, can be recognised due to their dark signature. The position, orientation and shape of new and old fractures are well evident in the image. The older are covered by grey ice, while the new are either ice free or covered by grease ice. Analysis of the number and width of fractures allow to concluded that the wind speed at this part of the Barents Sea is lower than in the Pechora Sea (compare with *Figure 6*). The i/b Kapitan Dranitsyn operated inside the covered area on April 27, and *in situ* observations demonstrated a fairly stable and homogenous ice situation in the area after the image acquisition.

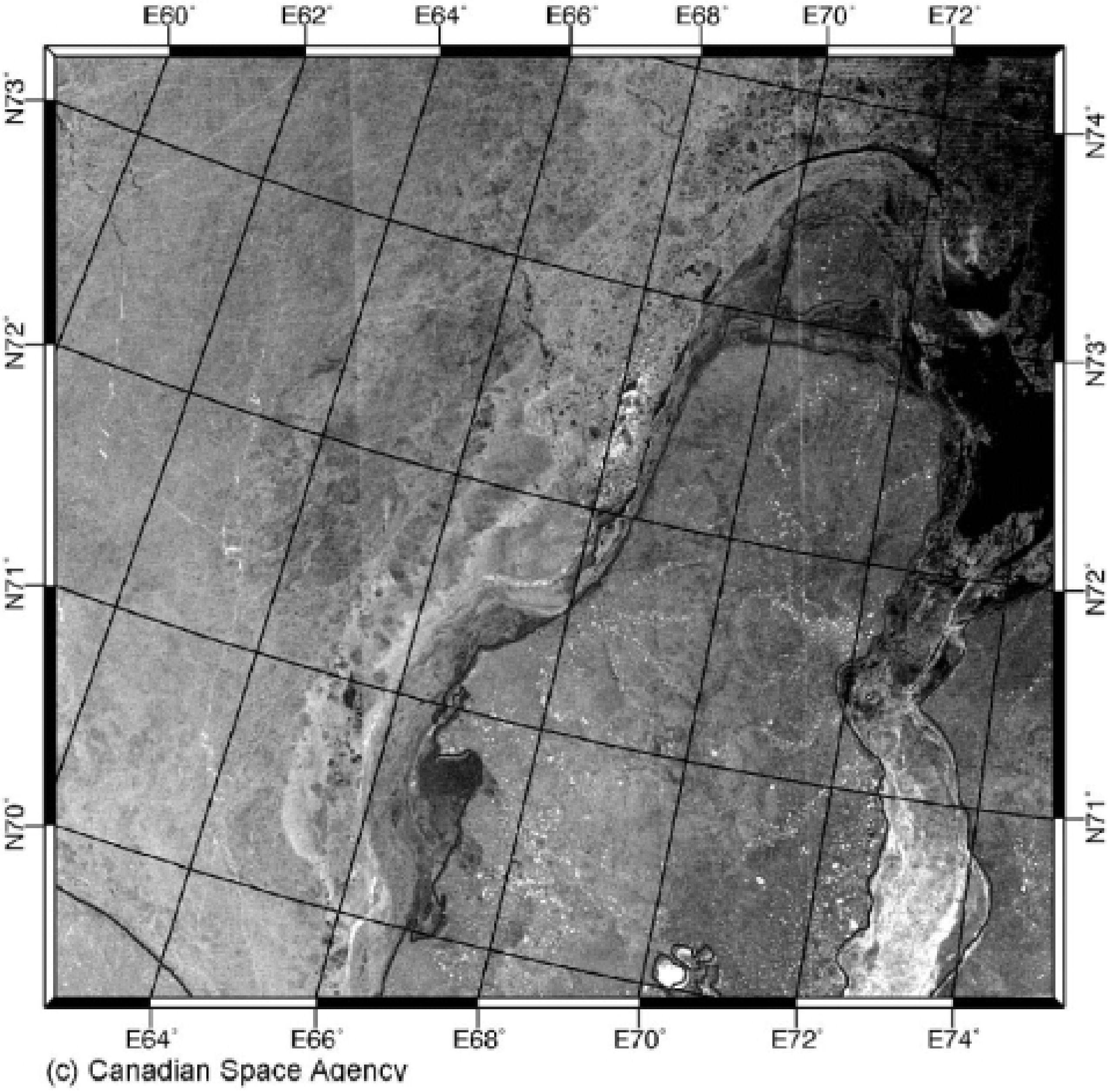

Figure 8. RADARSAT ScanSAR of April 25, 25 12:44 GMT, covering the Kara Sea, Yamal peninsula and Ob bay.

3.3 RADARSAT SCANSAR OF APRIL 25 12:44 GMT

The RADARSAT ScanSAR of April 25 (12:44 GMT) resolves the ice situation in the central and southwestern part of the Kara Sea, west of Yamal Peninsula. As measured on Cape Kharasavey the wind changed its direction from northwestern of April 23 to southeat on April 25. During the same period the air temperature dropped from between -11 to -13°C to between -15 to -19°C. The consequences of these weather changes on the ice conditions are evident in the image.

Depending on extent, thickness, and roughness, the fast ice will appear somewhat different in the image. Level ice has a dark signature, as is evident in the Ob estuary, where especially the northern part is covered by very level and rather thin ice. Deformed and ridged fast ice is mainly located along the western coast of the Yamal Peninsula, and around Bely Island. Bright signatures within the fast ice zones imply ridged and hummocked ice features.

The Yamalskaya recurring polynya is vast at the time of satellite observation and was recommended for ARCDEV sailing route. It is covered by grey and grey/white ice, but include also many giant and large consolidated ice floes. Areas with ice breccia that should be avoided when sailing can be identified in the SAR image. These features have different thickness and roughness because they have different origins, i.e. either from the Novaya Zemlya massif or the fast ice outside Cape Kharasavey.

Differences in the brightness signature of grey and grey/white ice and single first year ice floes are evident in the image. Several consolidated larger single first-year ice floes can be seen north and northwest of Bely Island. In the Kara Sea, areas with lighter ice conditions can be evaluated and recommended for route selection. Together with an ERS-2 scene of April 17, this image was used for recommendation of an optimal way through the fast ice in the Ob estuary. Based on the recommendations an channel was prepared by ni/b Vaygach, later used by the ARCDEV convoy to reach the gas deposit outside Sabeta/Tambey.

3.4 RADARSAT SCANSAR OF APRIL 25 12:45 GMT

The RADARSAT ScanSAR of April 25 (12:44 GMT) resolves the ice conditions from Cape Zgelanya to Bely Island. In addition to the vast Novozemylskaya recurring polynya, the image covers the northeastern part of the Barents Sea. The polynya is mainly covered by grey and grey/white ice, and was recommended for the navigation. Within the polynya the signature of the shiptrack of a convoy lead by ni/b Sovetskiy Soyuz can be seen as a diffuse thin bright line crossing 76°N at about 59°E. Comparison with the RADARSAT scene of April 23 reveals that the two large first year ice floes around 76°N have moved several km northwards. Due a very dark radar signature it is likely that the large polynya at Cape Zgelanya consist of open water.

The total amount of ridges, as well as the position, shape and general orientation of each separate ridge and fracture in the Novaya Zemlya ice massif can be resolved in the image. The possibility to retrieve such detailed ice parameters is one of the advantage of the SAR sensor. This kind information can be used to avoid zones of hummocked ice, and for selecting routes with relatively lighter ice conditions, for which this image is a good example.

The long line with dark signature directed southeastwards from Cape Zgelanya to Bely island is part of the routine sailing route in from Cape Zgelanya. In the image, this route contained a chain of fractures in the ice massif that could be utilised for ice navigation. Nevertheless, when the ARCDEV convoy reached this area on April 28, these fractures as well as the polynya outside Cape Zhelanya were closed, and a route going farther east and then southwards along the shores of Taymyr was chosen. Another sailing route goes along the eastern shores of Novaya Zemlya, but was not selected due the hostile ice conditions in the Novaya Zemlya ice massif.

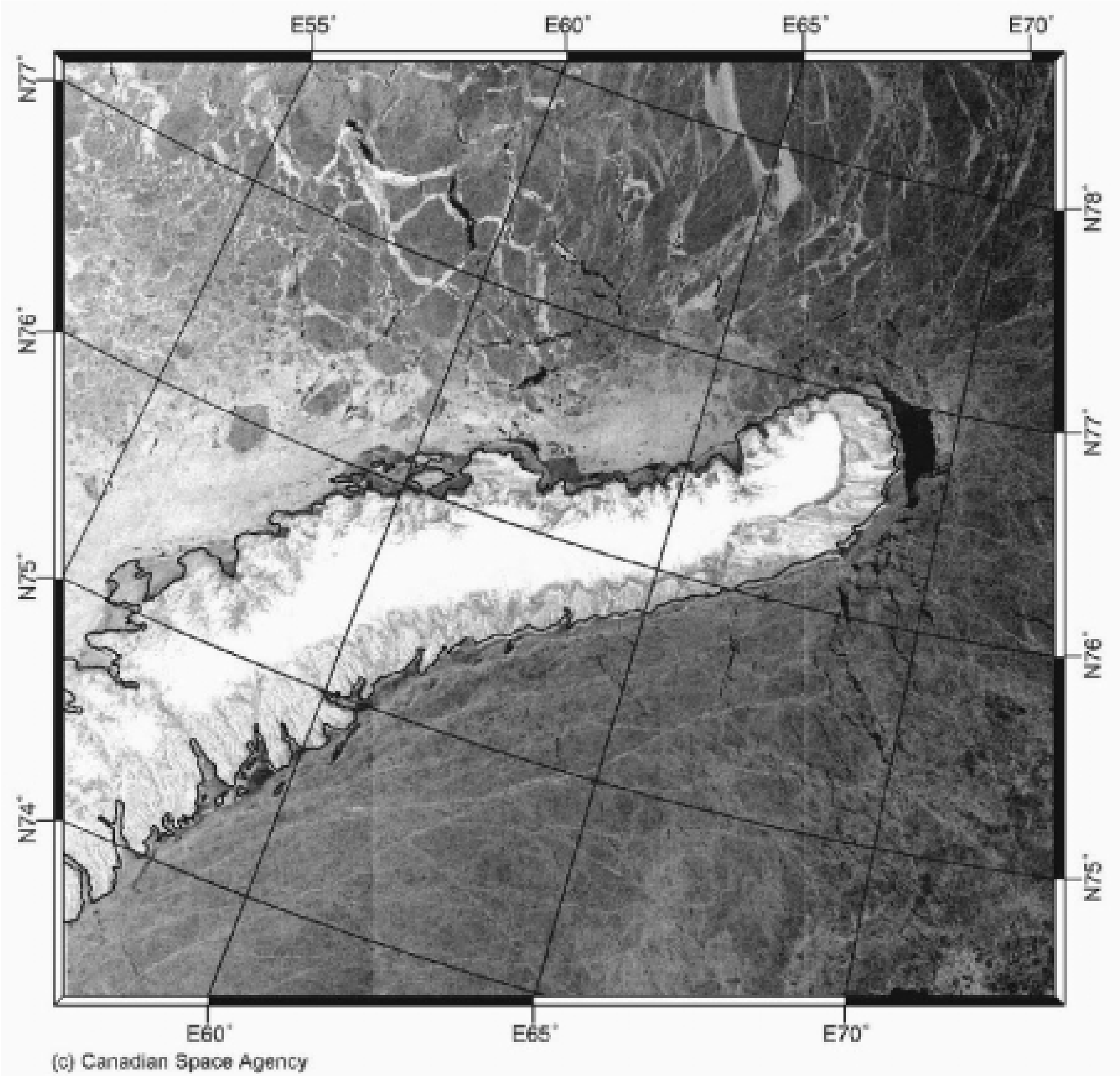

Figure 9. RADARSAT ScanSAR of April 25, 12:45 GMT, covering the northeast Novaya Zemlya, Barents Sea and Kara Sea.

3.5 RADARSAT ScanSAR of April 30 11:58 GMT

Due the ice situation north and northeast of Novaya Zemlya the common route from Cape Zhelanya to Bely island was not used. Analysis of satellite radar data allows for evaluation of the general direction of the fractures at the Cape Zgelanya region. The selected non-standard route going first directly eastwards, then south and westwards along the shores of Yamal has never been used in the winter-season before.

The RADARSAT ScanSAR of April 30 (11:58 GMT) resolves the ice conditions in the southeastern part of the Kara Sea along the shores of Taymyr and Yamal Peninsula. Due eastern and north-northeastern winds at the Kara Sea region in the period from April 25 to 30, both the Ob-Yeniseyskaya and Taymirskaya recurring polynyas were very large. The polynyas consisted of open water and/or new ice, as can be seen west and south of the AARI island (upper right corner of SAR image).

Areas with lighter ice conditions can be distinguished due to the very bright backscatter signal of grey ice, in contrast to the darker signature of weathered first year ice. In the drift ice several large and gigantic first year ice floes are identifiable, and were avoided in the routing selection.

Level land fast ice has a very dark radar signature, and is among others observed inside the Ob estuary, around the Sibiryakov Island, and northeastwards from Dikson. Farther into the estuaries the radar backscatter signal increases, as an effect of a rougher ice surface, and the absence of salt water. Tracks of icebreaking activities can be seen as thin bright lines both in the Ob and Yenisei estuaries.

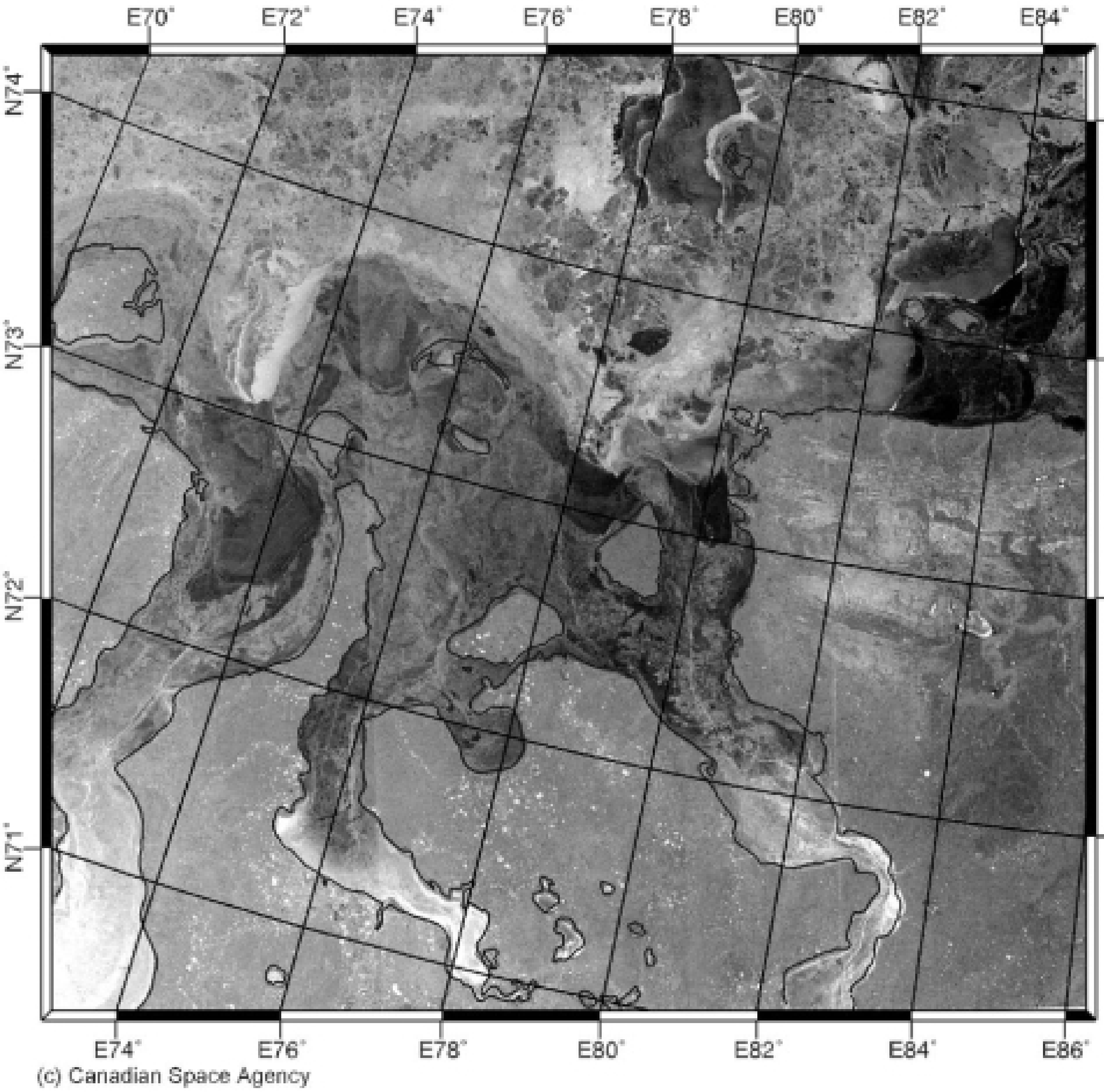

Figure 10. RADARSAT ScanSAR of April 30, 11:58 GMT, covering the central southern Kara Sea.

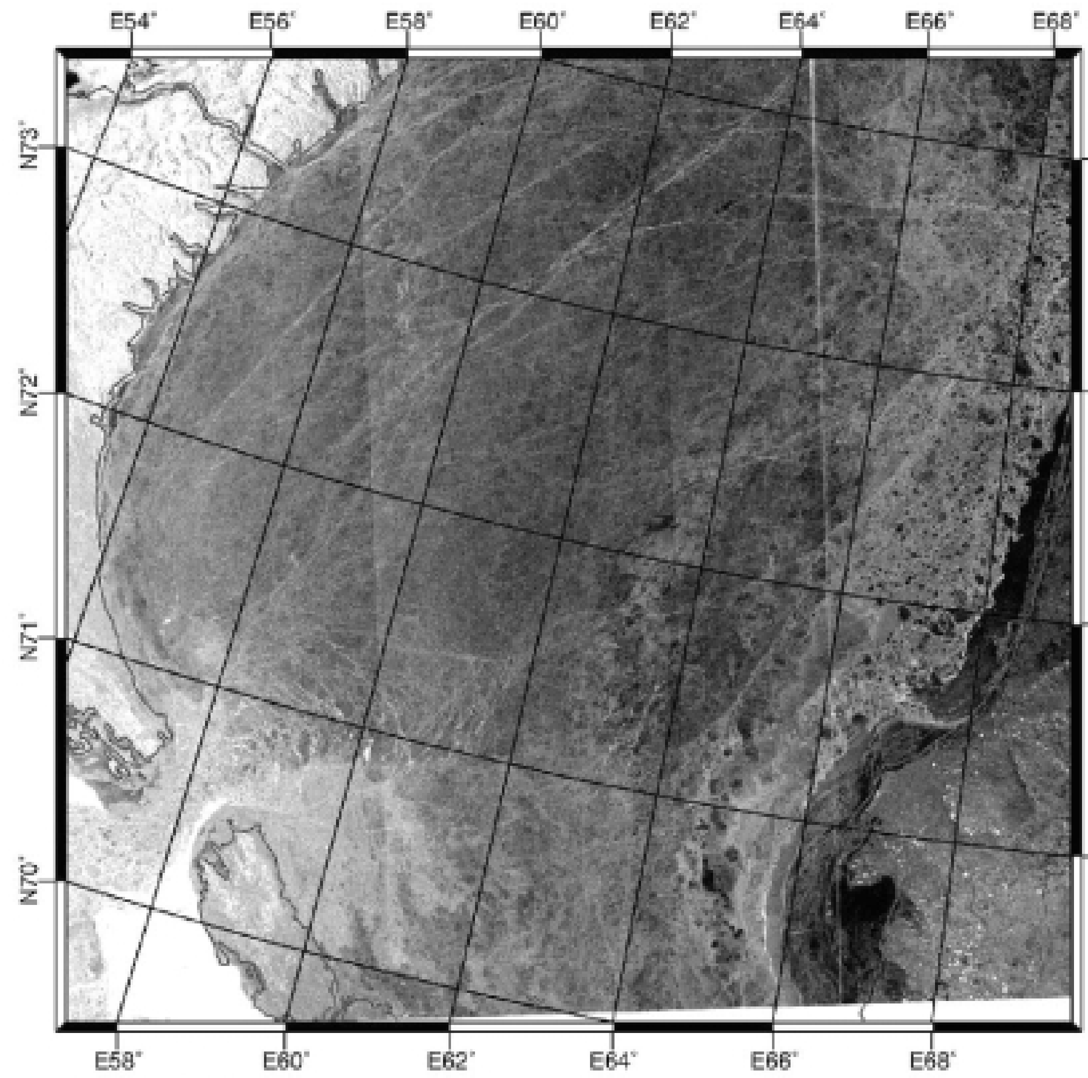

Figure 11. RADARSAT ScanSAR of May 8, 13:05 GMT, covering the western Kara Sea.

3.6 RADARSAT SCANSAR OF MAY 8 13:05 GMT

The RADARSAT ScanSAR of May 8 (13:05 GMT) was received onboard i/b Kapitan Dranitsyn 4 hours after acquisition and resolves the ice conditions in the southwestern part of the Kara Sea, in addition to small parts of the Pechora and Barents Sea. The image was important in the decision process for selecting the southern routing variant to the Barents Sea. As a result of the analysis sailing through the Kara Gate was preferred against using the Yugor Strait.

Analysis of weather information from the period prior to the image acquisition shows that wind changed its direction from southern on May 5 and 6, to eastern on May 7 and 8. This wind change started a deconstruction of the thick and compact first year ice at the Kara Gate region. The SAR image confirms these analysis. In the image the southern part of the Kara Gate is ice-free. From this area, a wind from the east with a speed of more than 12 m/s can be evaluated.

The drift ice of the Novozemelsky ice massif contains mainly thick and medium first-year ice, and grey and grey/white ice. Areas with difficult ice conditions such as ice breccia and ice blocks northeast of Vaygach Island and northwest of Cape Kharasavey, can be determined and avoided in the routing selection.

Comparison with the RADARSAT images of April 23 and 25, permits to evaluate the changing ice conditions at the Kara Gate, and along the western shores of the Yamal Peninsula. Crammed full and hummocked ice still surrounds Vaygach Island, although processes of fracturing and opening of the ice are seen.

Large areas with open water appear west and southwest of Vaygach Island, and along the southern shores of Novaya Zemlya. Fractures in the thick first year ice cover northeast of the Kara Gate can be recognised due to a very bright signature. Also evident in the image are ice motion processes from the Kara Sea to the Pechora Sea, which create lighter ice navigation conditions.

Fast ice is identified along the western shores of Yamal Peninsula and along the Novaya Zemlya Archipelago. Ridges, hummocks and level ice in the fast ice zone outside Cape Kharasavey can be identified and divided. Lighter ice conditions for loading operations of a convoy operating in the area at that time were proposed.

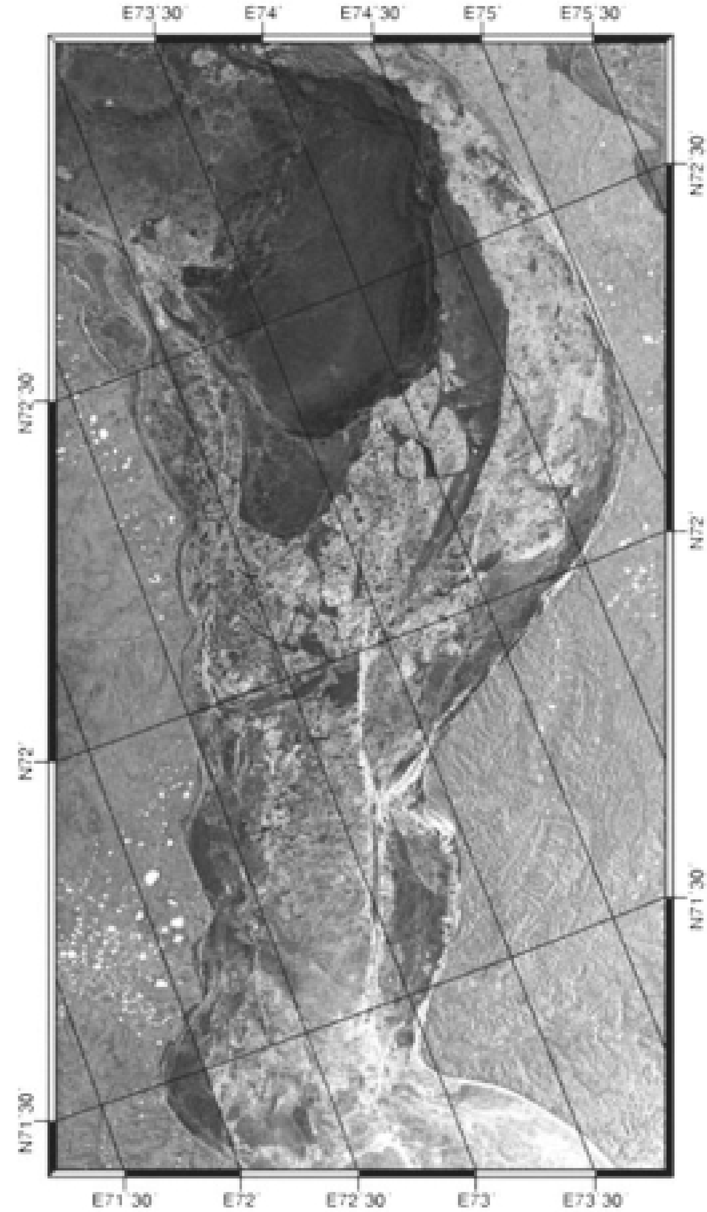

Figure 12. ERS-2 SAR of April 17, 06:47 GMT, covering the Ob estuary. © European Space Agency

3.7 ICE CONDITIONS IN THE OB ESTUARY AND PREPARATION OF AN ICE CHANNEL

Ice routing inside the Ob estuary is extremely hard, especially at the time of the late winter season for which ARCDEV took place. The main problem is the high concentration of hummocks in the river ice. Traditional optical and microwave satellite observation technologies cannot retrieve such ice parameters. Due the SAR sensor's high resolution and ability to penetrate dry snow and the upper layer of the ice cover the form and arrangement of fast ice and the hummocks are recognised and mapped.

Two ERS-2 SAR scenes of April 17 (06:47 GMT) resolves the fast ice condition in the Ob estuary. Level fast ice has a very dark radar backscatter signature, as is evident at the river mouth. Farther into the estuary the ice gets more ridged and hummocked, and the backscatter signature increases. Detailed analysis of the image was used to select an optimal sailing route through delineated areas with level and more easy ice conditions in-between the heavy deformed ice, to the loading location outside Tambey/Sabeta (71°18N/72°08E). A list with geographical positions for the most optimal route was send by fax to the captain of ni/b Vaigach, which prepared the ice channel. *In situ* observations collected later from Kapitan Dranitsyn confirmed the SAR analysis. MOH found the analysis a vital for the planning of the through the fast river ice in the Ob estuary.

3.8 ERS-2 SAR OF APRIL 25 07:35 GMT

This ERS2 SAR image (2.5 scenes) covers the ice conditions outside Cape Zhelanya on Novaya Zemlya, and was acquired about 5 hours before the RADARSAT ScanSAR image described in Chapter 3.4. In addition to the fast ice zones around the coast of Novaya Zemlya, weathered and consolidated pack ice floes dominates the image. The general direction of fractures and cracks useful for navigation can be identified, and the main orientation is north-north-eastward from Cape Zhelanya. The size, shape, position and distribution of larger first year ice floes are evident.

The most evident difference between the two satellite surveys is the significant different backscatter signatures of the large flaw polynya outside Cape Zhelanya. The low value measured by RADARSAT compared to ERS can be caused by a combination of several effects: 1) incidence angle of respectively 45° and 23°, 2) HH- vs. VV-polarisation, 3) formation of new ice and/or nilas during the 5 hours time difference and 5) decrease of wind speed and change to more along-track direction. Singly, all these effects will result in a lower backscatter signal. The presence of the 2 first is certain, while the two others can only be suggested. Accessible weather maps confirm the assumption that a deep cyclone passed the region early in the morning on April 25, while at noon the weather situation was calmer and colder. As a result there was a distinct change of the ice condition (hereby radar signature) at the flaw polynya. Other signatures and features are almost identically measured by the two satellite sensors. A slight difference of the shape and ice at the border of the flaw ploynya are caused by wind forced ice motion.

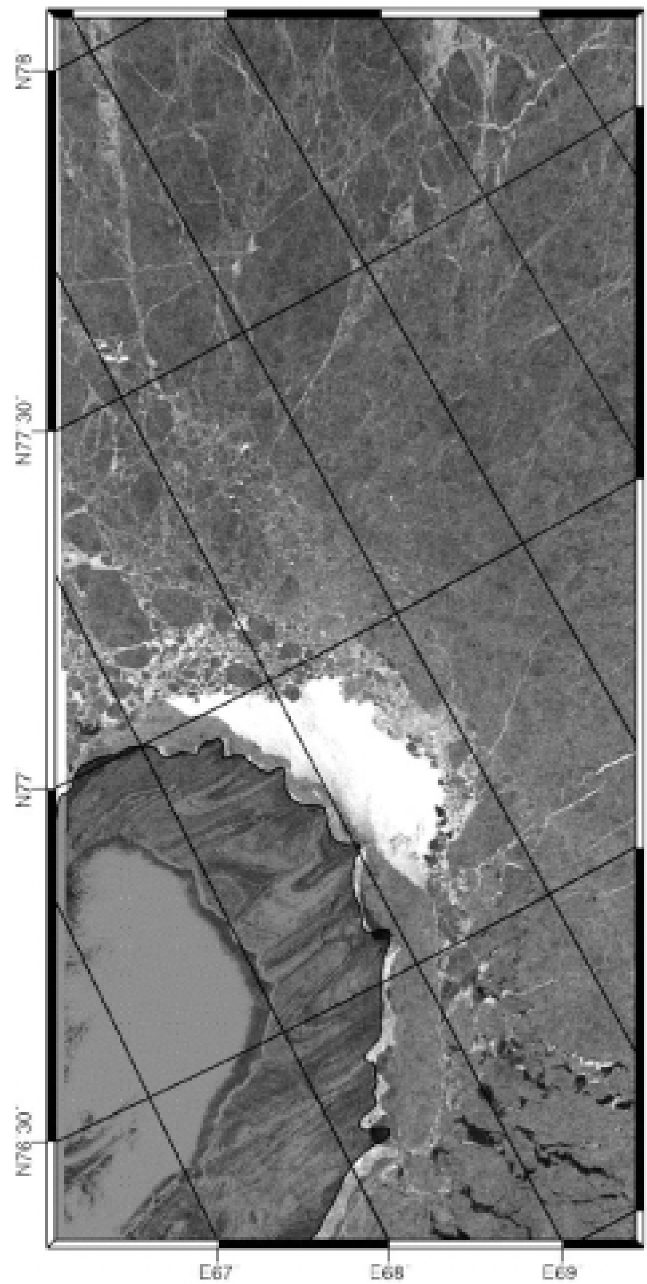

Figure 13. ERS-2 SAR of April 025 07:35 GMT, covering the northeastern Novaya Zemlya. © European Space Agency

3.9 ERS-2 SAR OF APRIL 29 07:09 GMT

This ERS-2 SAR image (3 scenes) was very important for the planning of the navigation route from Cape Zhelanya towards the Taymyr peninsula. The stripe covered a vast part of the interior of the northern Kara Sea ice massif, a region not covered by the pre-cruise ordered RADARSAT scenes. The ice situation is dominated by weathered thick and medium thick firstyear ice floes. Presumably, the identifiable fractures are covered mostly by nilas and grey ice. The general direction of cracks and fractures has changed from what was observed farther west, in the RADARSAT image of April 25. Here, the main orientation is from east to west, and from southwest to northeast, i.e. orientations unsuitable for the direction the convoy was heading. As result, the voyage had to take a long turn eastwards, before going south along the Taymyr peninsula.

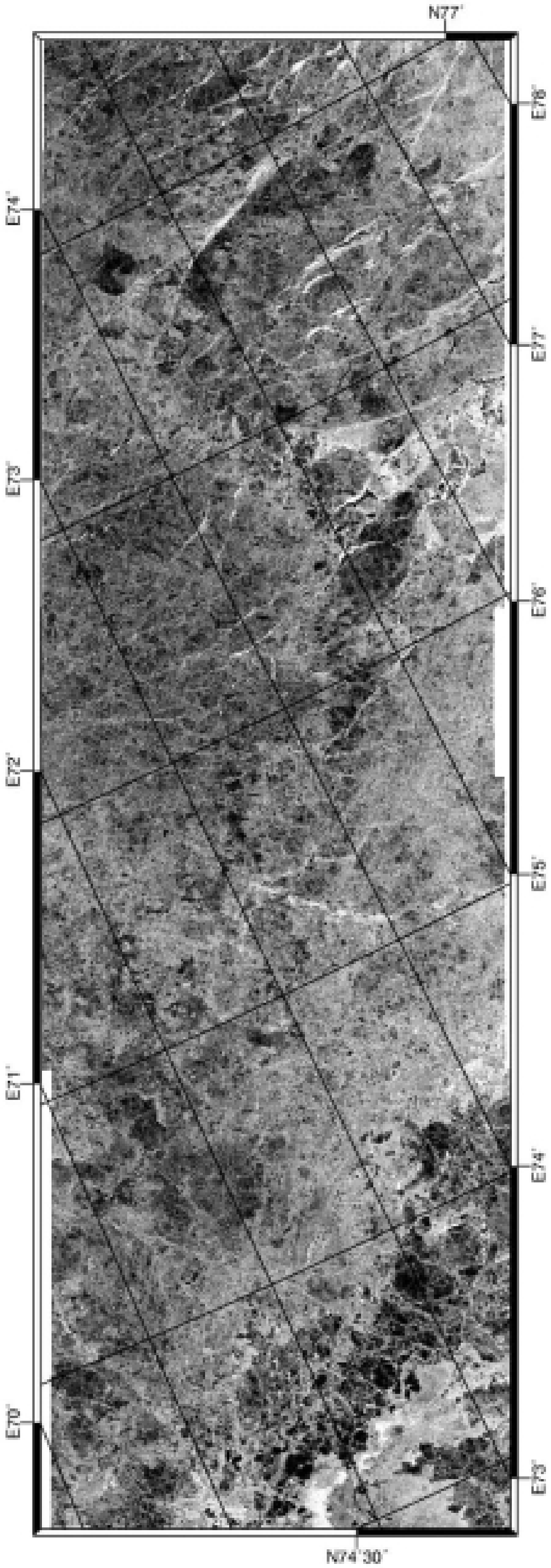

Figure 14. ERS-2 SAR of April 29, 07:09 GMT, covering the interior of the northern Kara Sea ice massif. © European Space Agency

3.10 ERS-2 SAR OF APRIL 30 06:38 GMT

This ERS-2 SAR image demonstrates the ice situation north-eastwards from the Gydan estuary, and was acquired about five and a half hour before the RADARSAT ScanSAR image described in Chapter 3.5. The ice features appear mainly the same in both images, except for a distinct difference in the radar backscatter signal of the flaw polynya west of AARI island. Level fast ice can be seen in the lower right of the image. In the lower part of the image, the size and distribution of larger first-year ice floes can be delineated within the areas with more light ice conditions.

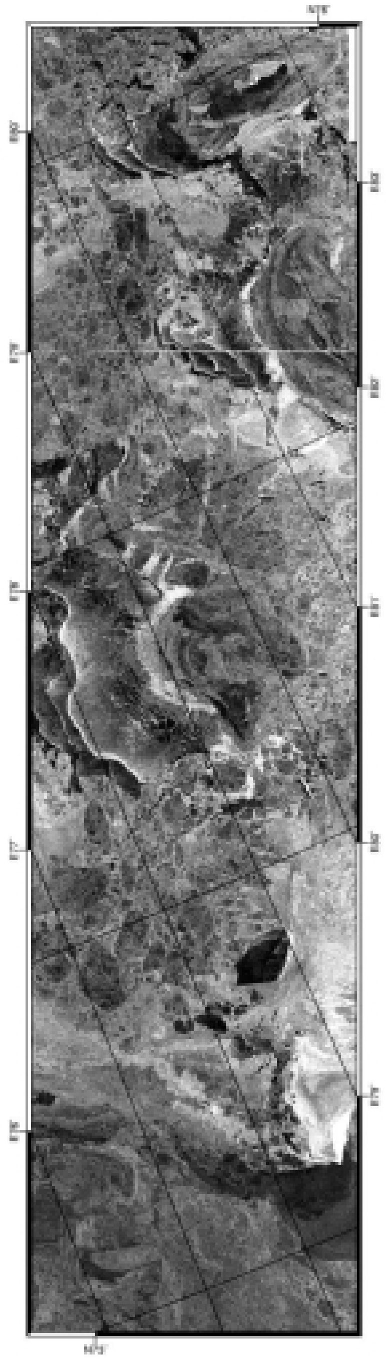

Figure 15. ERS-2 SAR of April 30, 06:38 GMT, covering the central southern Kara Sea and parts of the area also covered by RADARSAT ScanSAR 5 hours later. © European Space Agency.

3.11 ERS-2 SAR OF MAY 3 06:45 GMT

These ERS-2 SAR scenes demonstrate the ice distribution in the Ob estuary. In the fast ice zone, areas covered by level smooth ice (very dark signature) can be separated from areas with hummocked and ridged ice (grey and bright signatures). I/b Vaygach prepared an ice channel through areas with more easy ice conditions based on information from the analysis of the ERS-2 scene of April 17, and RADARSAT ScanSAR of April 25. The result of the icebreaking activity can be analysed in this image, where the channel can be seen as a very bright and linear thin line through the ice. We notice that the captain and pilots really selected an optimal way, with more light ice conditions. This means that MOH and NERSC/NIERSC recommendations for the i/b Vaygach route was correct.

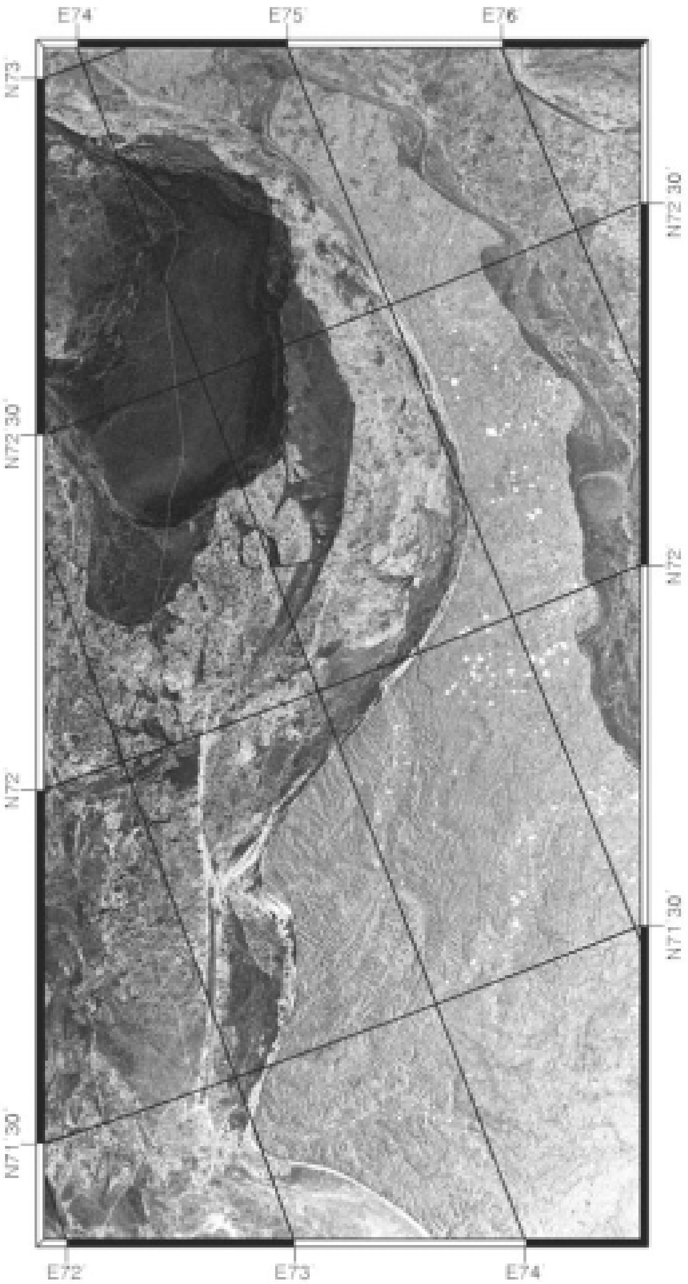

Figure 16. ERS-2 SAR of May 3, 06:45 GMT, covering the Ob bay. © European Space Agency

3.12 ERS-2 SAR OF MAY 6 06:50 GMT

These ERS-2 SAR scenes demonstrate the ice distribution in the Ob estuary, after i/b Kapitan Dranitsyn and tanker Uikku used the channel prepared by i/b Vaygach. The increased brightness signal from the channel compared with the image of May 3 is due to a new opening of the channel, caused by Kapitan Dranitsyn and Uikku's steering operation. In Figure 17 the white arrow show the destination area for the expedition. Kapitan Dranitsyn icebreaking operations outside Sabeta, in order to prepare an artificial harbour can also be seen. Field observations around the artificial harbour permits to validate the image brightness signatures of different ice types in the SAR image. Areas covered by level smooth ice will have a dark signature, while hummocked and ridged fast ice areas will have a mellow to bright signature. The images also allow for a reconstruction of the genesis of the ice cover of a large part of the estuary. The photos superimposed on Figure 17 are taken along the ARCDEV sailing route.

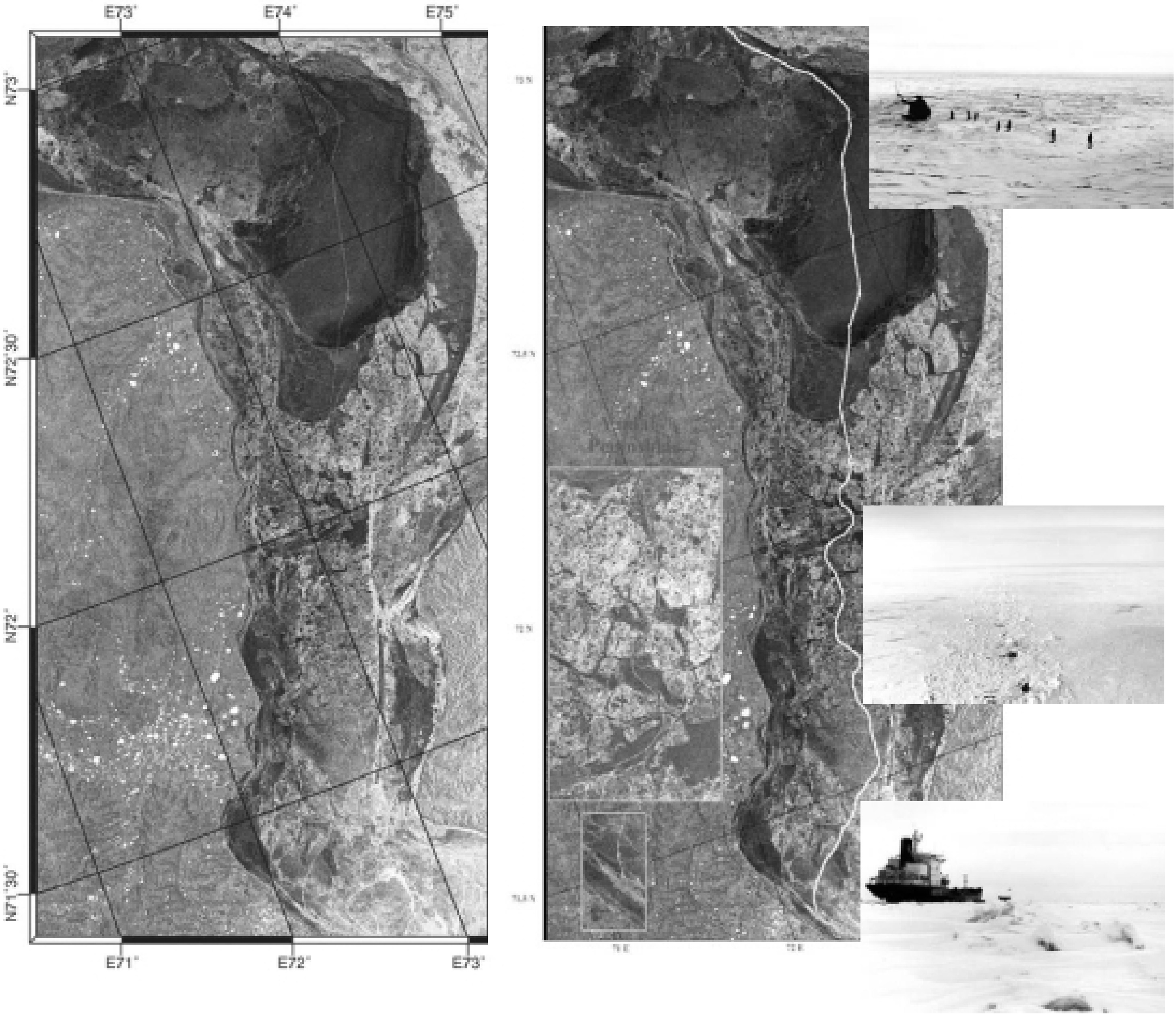

Figure 17. ERS-2 SAR of May 6, 06:50 GMT, covering the Ob bay. © European Space Agency

4 EFFECT OF IMAGE RESOLUTION

When satellite data are to be transferred digitally to icebreakers using satellite communication links such as for example INMARSAT, it is important that the image file size is kept as low as possible. At the edges of the ground coverage of the INMARSAT satellites (basically the whole Arctic) the transmission can be fragile, and thus the connection time should be as short as possible. An efficient way to reduce the file size, besides using file compression programmes, is to reduce the image resolution. This is done by adding and averaging two or more pixels, preferably the same number in each direction. As can be seen from Figure 18, the major information and features are preserved when the pixelsize is increased from 100m, to 250m to 500m. For a full RADARSAT ScanSAR scene, this means as reduction of the filesize from respectively 25 Mb, to 4 Mb, to 1 Mb. File compression programmes, such as JPEG, will reduce the filesize further, though also reducing the resolution and changing the initial pixel values. During the ARCDEV expedition a filesize of 250m was used, with additional reduction using JPEG-compression. These imagery contained enough information to be useful for the navigation support, for example did the convoy avoid several large and thick firstyear ice floes left of the middle in Figure 18.
New commercial compression techniques specially designed for satellite imagery are under development, such as Mr. Sid.

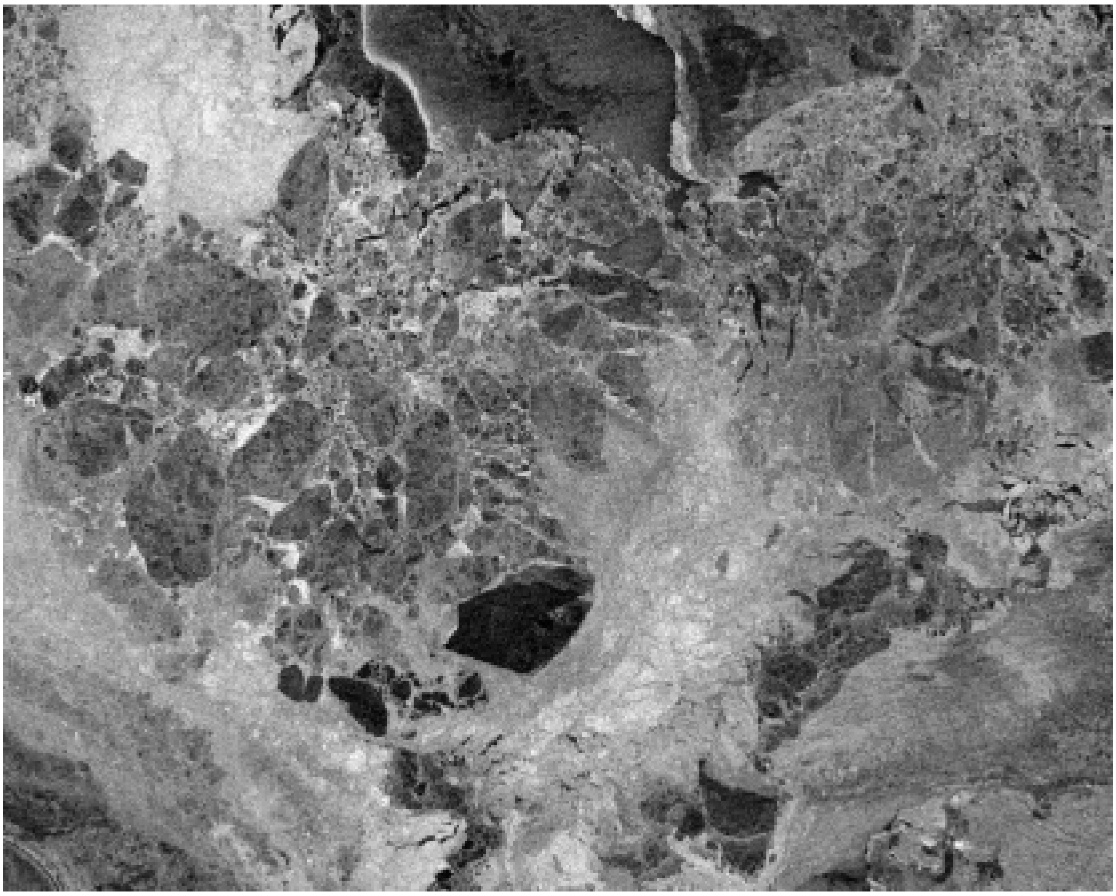

a)

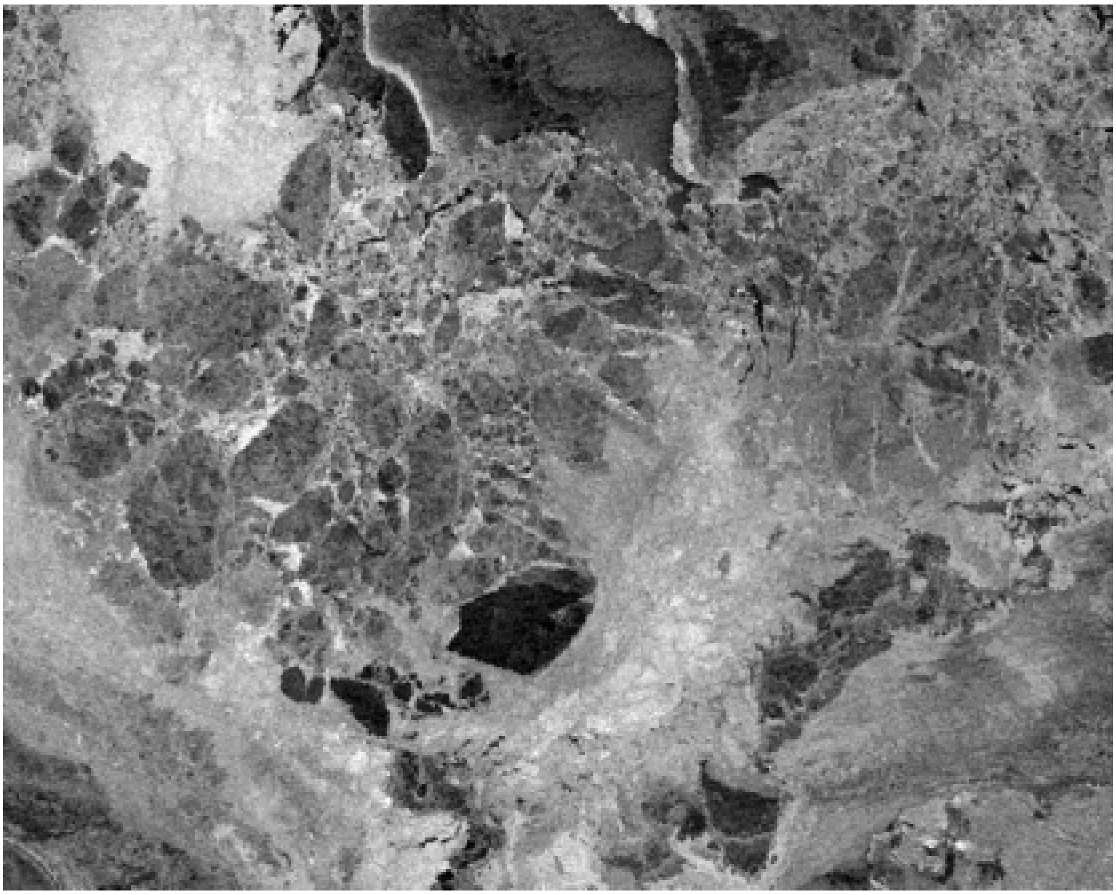

b)

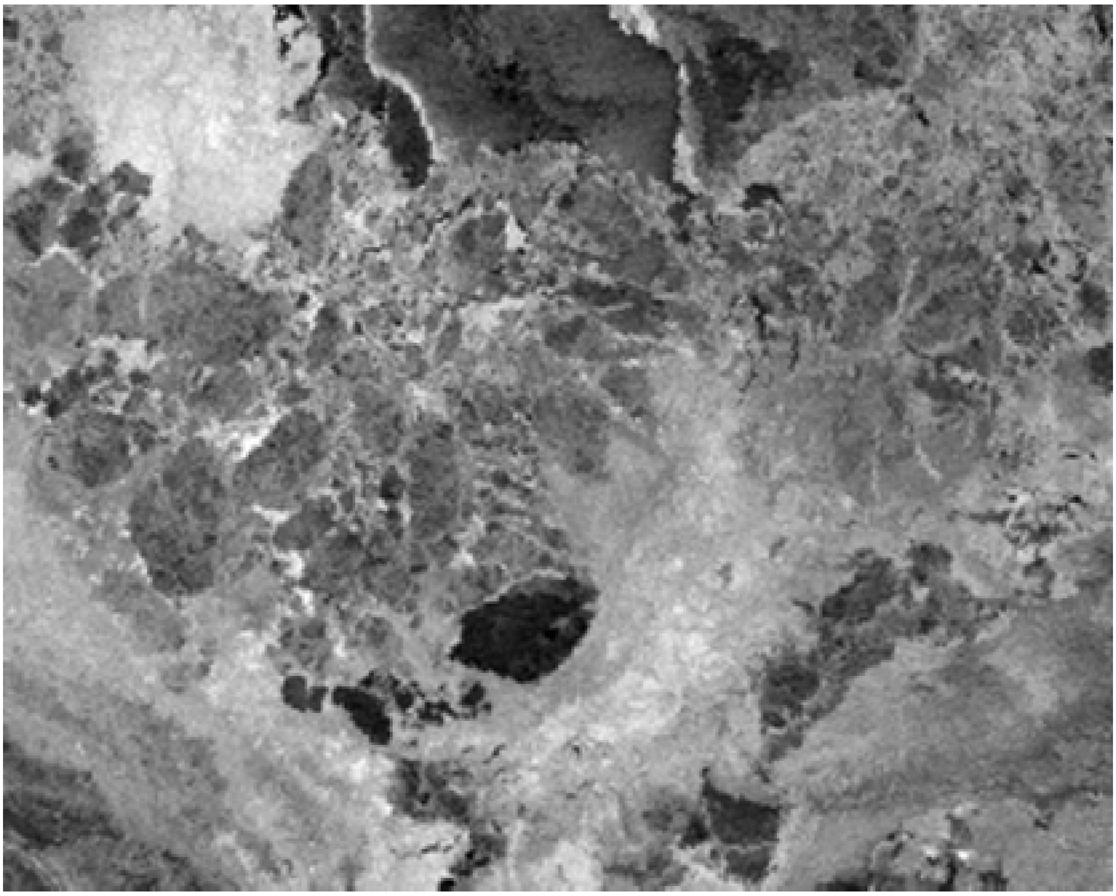

c)

Figure 18. The same sub-image, using a pixel size of a) 100m, b) 250m and c) 500m

5 COMPARISON OF RADARSAT AND IN SITU ICE OBSERVATIONS

5.1 COMPARISON OF RADARSAT SCANSAR AND VISUAL ICE OBSERVATIONS

In situ ice observations from i/b Kapitan Dranitsyn and ni/b Sovetsky Soyuz have been overlaid the RADARSAT ScanSAR images of April 30 and May 8. The SAR ice signatures and ice conditions are commented where it was possible or appropriate. The analysis has been performed on images with 250m resolution. As of today RADARSAT offers no absolute calibrated image products therefore a conversion to radar backscatter σ^0 values (dB) have not been done. The field observations from ni/b Sovetsky Soyuz were kindly provided through the ICE ROUTES project funded by the European Commission Transport RTD Programme of the 4th Framework Programme (Contract no. WA-96-AM-1136).

<u>Abbreviation:</u>
OW = open water
Ni = nilas
New = mainly a mixture of grease and nilas
G = grey ice
G/W = grey/white ice
FY = first year ice
C = ice concentration (0-10)

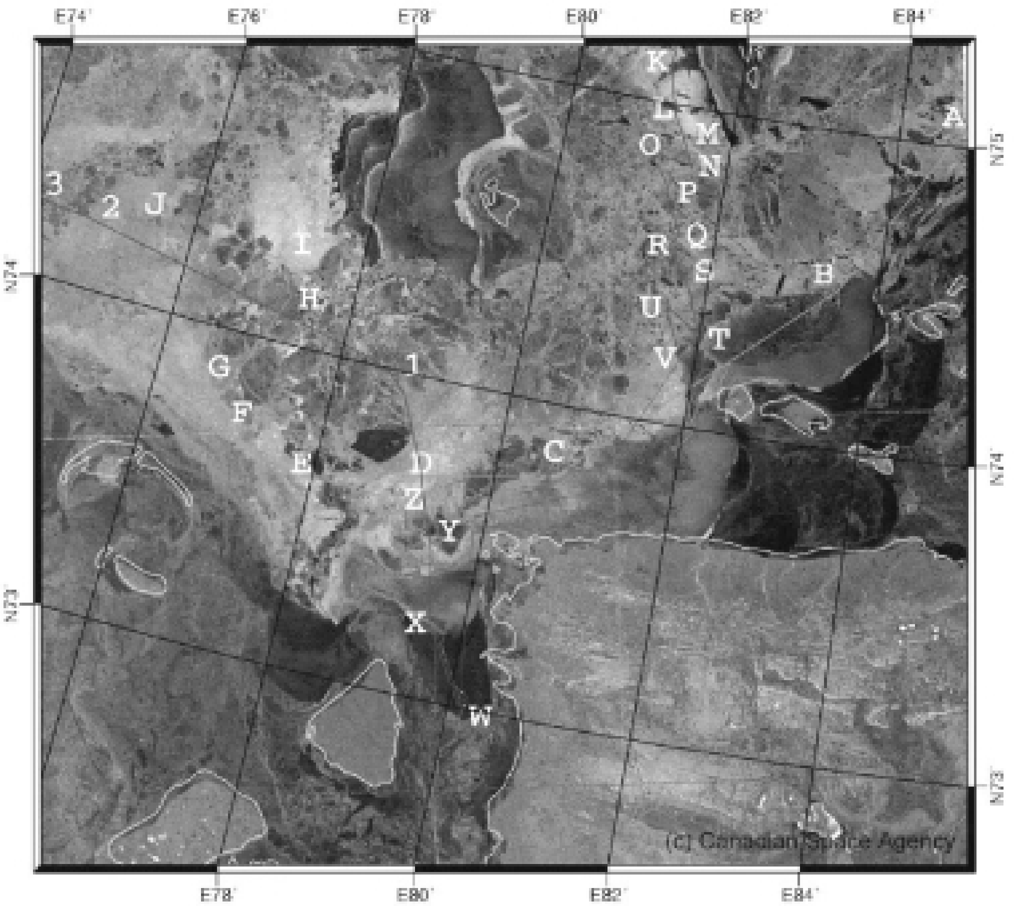

Figure 19. Sub-image 1 of RADARSAT ScanSAR of April 30.

COMMENTS TO SUB-IMAGE 1 OF RADARSAT SCANSAR IMAGE OF APRIL 30

Area A: 75°22N/85°25E		**In situ**: C=9-10, G/W (9), Ni (1), hummocks (2)
Comments: middle grey signature in the SAR image		
Area B: 74°30N/83°30E		**In situ**: C=9-10, G, G/W, Ni(6), FY med (3-4)
Comments: slightly dark signature tone, more nilas as even darker to the east		
Area C: 73°47N/80°40E		**In situ**: C=7-8, G, New
Comments: grey level increases, also change in texture		
Area D: 73°40N/79°00E		**In situ**: C=8-10, G
Comments: a slightly higher ice concentration may cause the brightness increase from C		
Area E: 73°42N/77°56E		**In situ**: C=9-10, FY med (5), FY thick (4-5), G, G/W (1-2), heavy ridging
Comments: more FY ice give more dark signature		
Area F: 73°50N/77°03E		**In situ**: C=9-10, FY thick (5), FY med (3), G, G/W (1-2), heavy riding
Comments: difficult navigation area		
Area G1: 73°53N/76°54E		**In situ**: C=8-9, G, G/W
Comments: A large FY floe the ship moved around		
Area G2: 73°55N/76°59E		**In situ**: C=8-9, FY thick (8-9), G/W (1), hummocks (2-3)
Comments: the large FY floe the ship moved around as dark area to the east.		
Area H: 74°08N/77°16E		**In situ**: C=9-10, FY thick (6), FY med (3), FY thin (1), small parts with river (brown) ice, hummocks (3-4)
Comments: somewhat dark signature due the FY ice		
Area I: 74°15N/77°07E		**In situ**: C=10, FY thick, med (6), FY thin (4), small parts with river ice, hummocks (2), close to ice belt
Comments: The ice belt can have moved, the edge between the to ice situations is well detected		
Area J: 74°15N/75°30E		**In situ**: C=9-10, FY thick (5), G/W (4-5), small parts with river (brown) ice, hummocks (2)
Comments: An area with a mixture of different ice types. G/W is the dominating ice feature.		
Area K: 75°10N/81°05E		**In situ**: OW, New, Ni, G
Comments: very dark signature from the new ice/open water (calm)		
Area L: 74°58N/81°15E		**In situ**: G, G/W, strongly rough FY 1 mile to the west
Comments: brighter signature, due to grey , grey/white ice, also note distinct texture		
Area M: 74°54N/81°24E		**In situ**: Narrow fracture covered with G, surrounded by strongly rough FY
Comments: can be the long and thin bright line		
Area N: 74°49N/81°32E		**In situ**: End of ice isthmus, OW fracture
Comments: difficult to determine		
Area O: 74°50N/81°08E		**In situ**: End of fracture, thick FY (7), thin FY (1), Young (1-2), strongly ridged and rough FY
Comments: here ni/b S.S. was stuck in the ice for 3 days		
Area P1: 74°45N/81°17E		**In situ**: Mean, thick FY (7), thin FY (2-3), Young (0-1)
Comments: similar signature as above		
Area P2: 74°40N/81°24E		**In situ**: Thick FY (8), mean FY (2), mean roughness, icecake
Comments: similar signature as above		
Area Q: 74°36N/81°33E		**In situ**: Fracture with OW and NI
Comments: may be too small to be seen in this image.		
Area R: 74°33N/81°27E		**In situ**: FY (6), G (3), fracture
Comments: a bit brighter than the observations under O and P		

Area S1: 74°28N/81°42E		**In situ**: G, ridged FY to the left and right
Comments: most important floes detected		
Area S2: 74°25N/81°48E		**In situ**: Fracture with OW and Ni
Comments: Between S and T it is mainly Nilas		
Area T: 74°18N/81°57E		**In situ**: Beginning of polynya
Comments: Border of polynya well detected, it consists of either new ice or open water. The bright signature at the edge can be pancake ice		
Area U1: 74°22N/81°33E		**In situ**: FY (1), G (6), G/W (2), fractures with OW
Comments: fractures difficult to see/determine in the SAR image		
Area U2: 74°19N/81°38E		**In situ**: G, G/W (2), OW to the west
Comments: water difficult to see/determine, especially without wind information.		
Area V: 74°13N/81°47E		**In situ**: Mix of Ni and Pancake near ice edge, close to polynya with OW
Comments: quite bright signature, the edge is not very distinct in the image		
Area W: 73°00/80°07E		**In situ**: Level Fast ice.
Comments: very dark, and similar to calm open water.		
Area X: 73°13N/79°40E		**In situ**: Unstable Fast ice, FY ice cake frozen together, close to ice edge zone and OW
Comments: brightness increase.		
Area Y: 73°28N/79°28E		**In situ**: Ni (7), G ice cake (3)
Comments: Dark tone for nilas, while the grey ice appears much brighter		
Area Z1: 73°38N/79°15E		**In situ**: Rafted Ni (3-4)
Comments: quite dark signature		
Area Z2: 73°43N/79°09E		**In situ**: G (5), Ni (4)
Comments: brightness increases some		
Area 1a: 73°56N/78°47E		**In situ**: Young ice, G/W (4), G (4), Ni (1), few ridges
Comments: mellow brightness		
Area 1b: 74°01N/78°21E		**In situ**: FY (1-2), G/W (5), G (3)
Comments: slightly more dark		
Area 2: 74°12N/75°07E		**In situ**: Thin FY, G/W, close to polynya with G/W
Comments: mellow brightness, but is difficult to judge due the ice drift.		
Area 3: 74°14N/74°08E		**In situ**: Thin FY (6), G/W (3), Ni (1), fractures
Comments: difficult to judge due the ice drift		

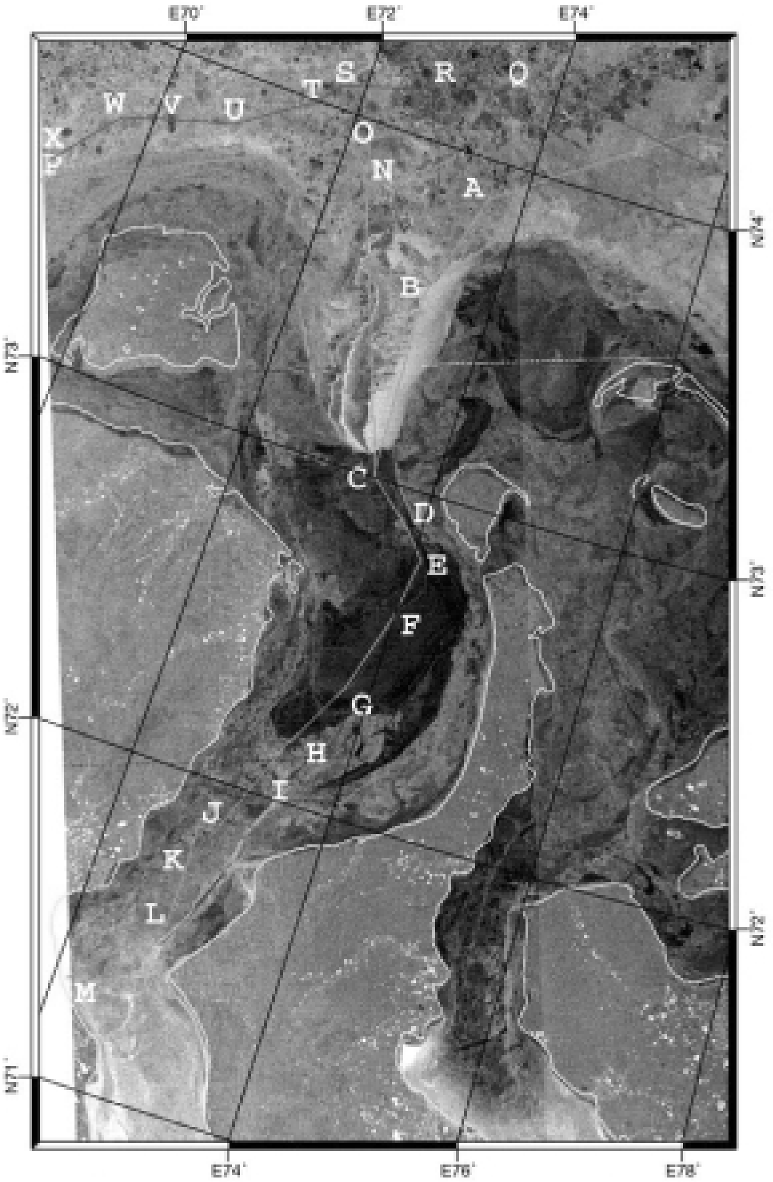

Figure 20. Sub-image 2 of RADARSAT ScanSAR of April 30

COMMENTS TO SUB-IMAGE 2 OF RADARSAT SCANSAR SCENE OF APRIL 30

Area A: 73°53N/73°37E		**In situ**: C=5, G, G/W, large areas with OW
Comments: low concentration may cause the somewhat darker signature of G than seen before		
Area B: 73°34N/73°20E		**In situ**: C=9-10, FY thick (6), G/W (3-4), hummocks (2-3)
Comments: hummocking may cause the very bright signal in this area		
Area C: 73°00N/73°22E		**In situ**: C=10, Fast FY ice (50 cm), River (brown) ice, smooth surface, dust on surface, hummocks (2), snow (2)
Comments: signature level comparable to that of calm open water		
Area D: 72°53N/73°52E		**In situ**: C=10, Fast FY ice, med. thickness
Comments:		
Area E: 72°48N/74°05E		**In situ**: C=10, Fast FY ice
Comments: the ship-track of ni/b Vaygach can be seen as a thin bright line on the very dark signature of level fast ice.		

Area F: 72°38N/74°00E		**In situ**: C=10, Fast ice, thickness = 1.20m, brackish water, river ice, brown water
Comments:		
Area G: 72°27N/73°51E		**In situ**: C=10, Fast FY ice,
Comments:		
Area H: 72°11N/73°24E		**In situ**: C=10, Thick Fast FY ice (1.5m), smooth surface, hummocks
Comments: beginning of area with more hummocked surface		
Area I: 72°04N/73°15E		**In situ**: Fast FY ice, smooth surface, hummocks
Comments:		
Area J: 71°51N/72°52E		**In situ**: C=10, thick Fast ice, hummocks (2-3), snow (2)
Comments:		
Area K: 71°43N/72°51E		**In situ**: C=10, Fast FY, mix of smooth and rough surface, hummocks 0.5-1m in height, brackish/ nearly fresh water
Comments:		
Area L: 71°33N/72°50E		**In situ**: C=10, smooth Fast FY ice, huumocks/sastrugi
Comments:		
Area M: 71°18N/72°09E (Sabeta/Tambey)		**In situ**: C=10, Fast FY ice, thickness >2m, hummocks (2-3) 0.5-1.5 m in height, artificial harbour/loading-station
Comments:		
Area N: 73°51N/72°16E		**In situ**: C=7-8, Ni, G, G/W, floesize 100-200m
Comments: difficult to judge**,** due to the ice-drift.		
Area O: 73°54N/72°03E		**In situ**: C=8-9, FY, edge between young and FY ice, thickness 1m
Comments: this edge cannot be recognised in the image, and has most presumably moved or disappeared		
Area P: 73°30N/69°07E		**In situ**: Thick mean FY (5), Young (4), mean roughness
Comments: difficult to judge**,** due to the ice-drift.		
Area Q: 74°13N/73°29E		**In situ**: Thick, mean FY (8-9), Ni (1), strongly rough
Comments: distinct mellow greyness for FY ice, several larger floes can be seen		
Area R: 74°09N/72°44E		**In situ**: FY ice (8), fractures with Ni (2)
Comments: similar as above		
Area S: 74°04N/71°45E		**In situ**: FY ice isthmus (2-3 miles), then FY(7), New, Young (3)
Comments: the isthmus cannot be seen with this resolution.		
Area T: 74°00N/71°34E		**In situ**: Thick, mean FY (6-7), Young (2-3), strongly rough
Comments:		
Area U: 73°51N/70°48E		**In situ**: Thick, mean FY (7), New, Young (2-3)
Comments:		
Area V: 73°48N/70°11E		**In situ**: Thick, mean FY (7), thin FY (3), strongly ridged
Comments:		
Area W: 73°45N/69°40E		**In situ**: Thick, mean FY (6), thin FY (2), G/W (2), strongly ridged
Comments:		
Area X: 73°33N/69°07E		**In situ**: Thick, mean FY (5), Young (4), mean roughness
Comments:		

Figure 21. Sub-image 1 of RADARSAT ScanSAR of May 8.

COMMENTS TO SUB-IMAGE 1 OF RADARSAT SCANSAR IMAGE OF MAY 8

Area A: 73°19N/68°06E		**In situ**: Thin FY, Ni, G, G/W (K.D)
Comments: This was an area with small floes and leads, and great variations in the ice types, in which the i/b could move fast. The edge of the thicker ice massif to the west is recognised well (ca. 67°30E). A significant amount of the ice floes are detected		
Area B: 72°48N/67°37E		**In situ**: thick FY (8), Grey (1-2) (K.D)
Comments: Presumably, the i/b- observation was made within the large dark floe, the surrounding ice are of the same character as in A.		
Area C: 72°10N/67°22E		**In situ**: Thick FY, ridged (K.D)
Comments: The observation is within a large floe, and the surrounding ice is a mixture of thick FY and Young ice.		
Area D: 72°07N/64°21E		**In situ**: Thick FY (9-10), Ni (0-1), heavy ridging (1-2m) (K.D)
Comments: This was a very difficult area, where the i/b had trouble getting through. The observation is within a very large segment (close 100km) which can be viewed as one giant floe, appearing with a quite dark signature in the SAR image. Areas of more broken FY ice within this floe is reasonable		

Area E: 73°16N/68°48E		**In situ**: OW, Ni (S.S)
Comments: An area with large variations of ice features, in which the i/b could move fast. This observation is 2 days before the image was taken, so the ice can have become thicker and the amount of open water smaller (as compared with A)		
Area F: 72°58N/68°15E		**In situ**: ice cake, thick mean FY (6), new/young (3) (S.S)
Comments: less homogenous than E, may be caused by larger mixture of different ice features		
Area G: 71°24N/66°07E		**In situ**: G/W, few ridges (S.S)
Comments: somewhat more smoother texture than seen above		
Area H: 71°10N/65°19E		**In situ**: polynya (1km), mean, rough FY surrounding (S.S)
Comments: the localisation of the polynya is difficult to determine, can have closed since the observation was made (2 days separation).		
Area I: 71°04N/64°50E		**In situ**: thick, mean FY (7), young (2) (S.S)
Comments: mellow brightness		
Area J: 70°57N/64°11E		**In situ**: thick, mean FY, mean roughness, fractures (S.S)
Comments: similar as above, but the fractures cannot be seen with this resolution		

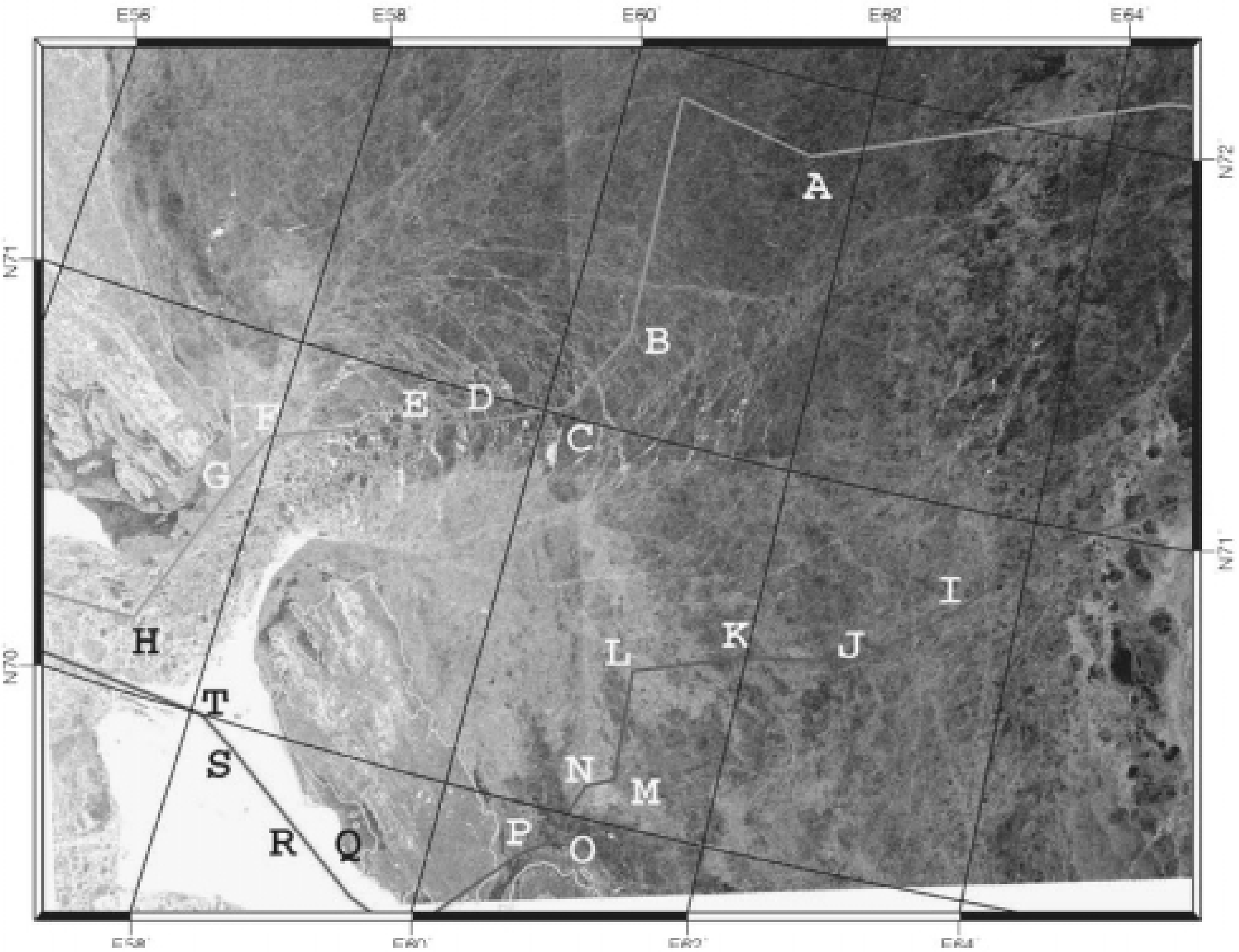

Figure 22. Sub-image 2 of RADARSAT ScanSAR of May 8

COMMENTS TO SUB-IMAGE 2 OF RADARSAT SCANSAR IMAGE OF MAY 8

<table>
<tr><td>Area A: 71°48N/61°35E</td><td></td><td>In situ: Thick FY (1.5m), h. ridges 0.5m, 100m int.</td></tr>
<tr><td colspan="3">Comments: 6-hours stop for K.D. Level to slightly ridged surface. Inside the Kara sea ice massif, a giant rigid ice element moving back and forth the coasts of Yamal peninsula and Novaya Zemlya</td></tr>
<tr><td>Area B: 71°14N/60°30E</td><td></td><td>In situ: Thick FY (9-10), Ni/OW (0-1), h. ridges 0.5-1m, small floes (</td></tr>
<tr><td colspan="3">Comments: The thin very bright lines can be either open water or large ridges, difficult to judge without better resolution and additional information.</td></tr>
<tr><td>Area C: 71°01N/60°09E</td><td></td><td>In situ: Thick FY, ridges, small floes</td></tr>
<tr><td colspan="3">Comments: Here begins the area of very thick and ridged FY ice, which lasted through the whole Kara Gate. Both ridge height and amount increases towards the Kara Gate.</td></tr>
<tr><td>Area D: 70°55N/59°29E</td><td></td><td>In situ: Thick FY (9-10), h. ridges 0.5-1m, int. 100m</td></tr>
<tr><td colspan="3">Comments: Same situation as above</td></tr>
<tr><td>Area E: 70°53N/59°03E</td><td></td><td>In situ: Thick FY (9), h. ridges 1-2m, floes >100m</td></tr>
<tr><td colspan="3">Comments: Similar situation as above, but the height and degree of ridging are increasing. The beginning of a very dynamic area.</td></tr>
<tr><td>Area F: 70°44N/57°58E</td><td></td><td>In situ: Thick FY (>2m), very ridged, distr. in all directions, h. 2-3m</td></tr>
<tr><td colspan="3">Comments: More ridged and deformed ice increases the brightness signature</td></tr>
<tr><td>Area G: 70°36N/57°49E</td><td></td><td>In situ: Thick FY (9), very ridged, h. 1-3m, small leads</td></tr>
<tr><td colspan="3">Comments: same as above</td></tr>
<tr><td>Area H: 70°11N/57°22E</td><td></td><td>In situ: G, G/W, OW</td></tr>
<tr><td colspan="3">Comments: Similar signature but different ice than observed above, may be caused by ice drift between SAR and in situ observations, data on the weather situation is needed. Rather easy ice navigation area.</td></tr>
<tr><td>Area I: 70°43N/63°28E</td><td></td><td>In situ: thick, mean FY, mean roughness</td></tr>
<tr><td colspan="3">Comments: somewhat more easy ice situation than was observed from Kap. Dranitsyn.</td></tr>
<tr><td>Area J: 70°33N/62°50E</td><td></td><td>In situ: thick, mean FY, mean roughness, fractures</td></tr>
<tr><td colspan="3">Comments: the fractures is not easy to determine with this resolution</td></tr>
<tr><td>Area K: 70°30N/61°58E</td><td></td><td>In situ: Rather level FY</td></tr>
<tr><td colspan="3">Comments: no apparent brightness signature difference from above.</td></tr>
<tr><td>Area L: 70°24N/61°10E</td><td></td><td>In situ: slightly rough FY, fractures</td></tr>
<tr><td colspan="3">Comments: here a distinct increase in the brightness signature from above</td></tr>
<tr><td>Area M: 70°07N/61°14E</td><td></td><td>In situ: thick FY, strongly rough</td></tr>
<tr><td colspan="3">Comments: The boundary between level and ridged/deformed FY is well determined. .</td></tr>
<tr><td>Area N: 70°05N/61°02E</td><td></td><td>In situ: fracture</td></tr>
<tr><td colspan="3">Comments: Consists mainly of FY ice, the fractures cannot be immediately seen.</td></tr>
<tr><td>Area O: 69°55N/60°52E</td><td></td><td>In situ: thick, mean FY, ridged</td></tr>
<tr><td colspan="3">Comments:</td></tr>
<tr><td>Area P: 69°52N/60°40E</td><td></td><td>In situ: fast ice boundary</td></tr>
<tr><td colspan="3">Comments: the fast ice boundary is distinct. The ship-track of Sovetsky Soyuz can be seen as a thin very bright line in the level fast ice.</td></tr>
<tr><td>Area Q: 69°39N/59°32E</td><td></td><td>In situ: OW</td></tr>
<tr><td colspan="3">Comments: difficult to judge without wind information</td></tr>
<tr><td>Area R: 69°47N/59°00E</td><td></td><td>In situ: G/W</td></tr>
<tr><td colspan="3">Comments: Difficult to judge due to ice drift and lack of synoptical data.</td></tr>
<tr><td>Area S: 69°56N/58°24E</td><td></td><td>In situ: compressed pancake</td></tr>
<tr><td colspan="3">Comments: Can be pancake ice, or open water with high wind</td></tr>
<tr><td>Area T: 70°00N/58°05E</td><td></td><td>In situ: FY (7), Ni (2), very rough</td></tr>
<tr><td colspan="3">Comments: The edge of the polynya can have moved westwards due to wind from the east. It is reasonable with FY ice at the edge. The actual edge is well detected.</td></tr>
</table>

5.2 COMPARISON OF RADARSAT SCANSAR AND PHOTOGRAPHS

Positioned photographs of the observed sea ice features were taken all along the route during the expedition. Here we present a comparison between RADARSAT ScanSAR signatures and photographs of some of the most dominating sea ice features observed. The image of April 30 is used for this study, with an image pixel resolution of 250*250m.

Figure 23. Radarsat SAR signature of very thick and heavy ridged firstyear ice observed at the Kara Gate. The height of the ridges was from 2-4 meters. Due to the heavy ridging this firstyear ice area is much brighter than an average firstyear ice area.

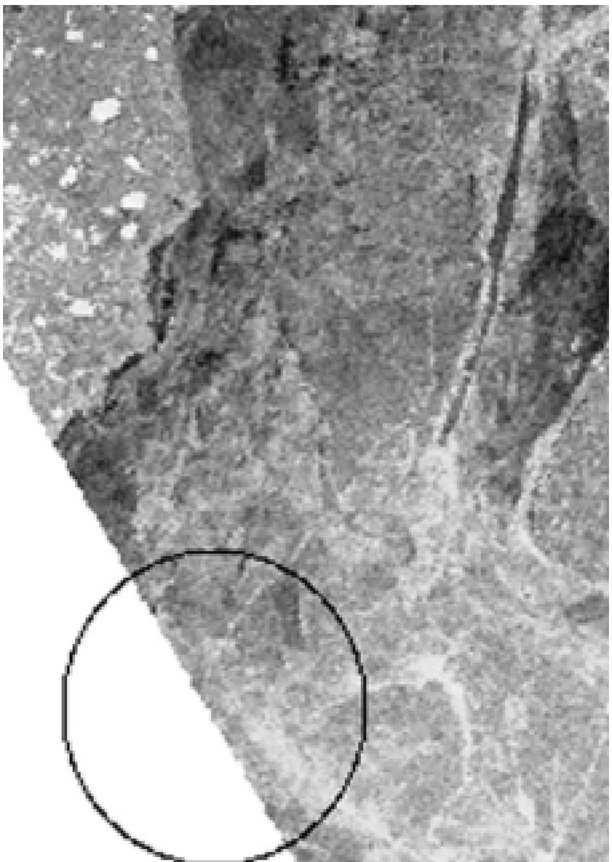

Figure 24. RADARSAT ScanSAR signature of hummocked fast ice observed in the Ob estuary. The height of the hummocks was less than 1 meter.

is

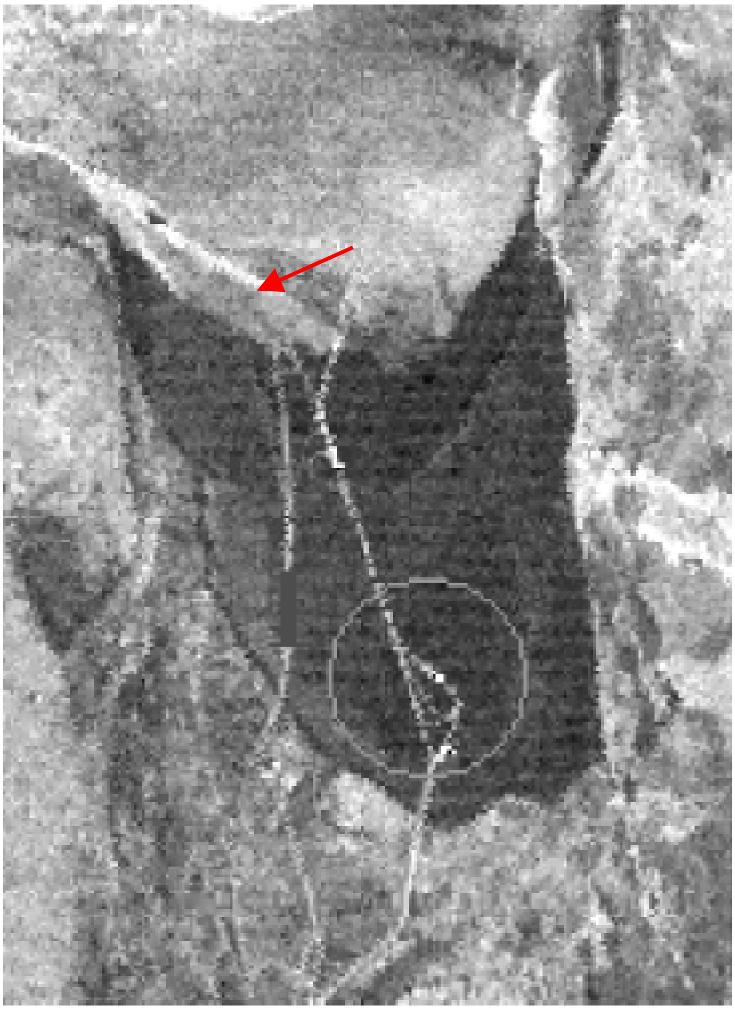

Figure 25. RADARSAT ScanSAR signature of level fast ice in the Yenisei estuary. The snow layer approximately 15 cm thick, and covers major parts of the sea ice surface. In the SAR image, two ship-tracks can be seen as very bright lines on the dark level fast ice signature. The red arrow points to a region with unstable fast FY ice (broken and then refrozen, hence the increased brightness signature).

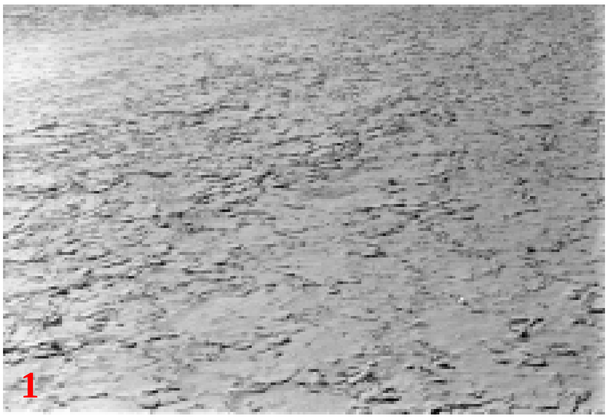

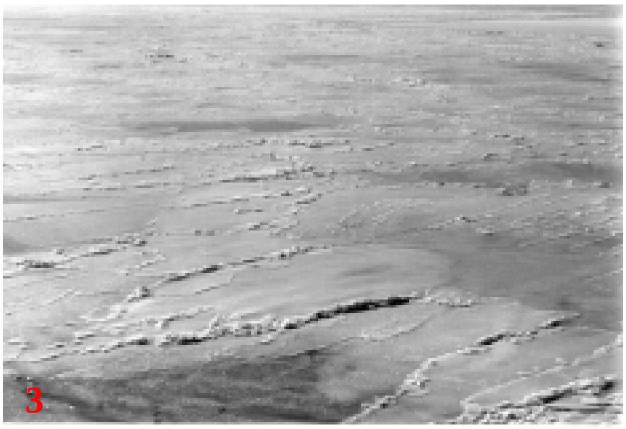

Figure 26. RADARSAT ScanSAR signatures of 1) Grey/white ice, 2) slightly ridged/deformed FY ice, and 3) Nilas, located west of AARI island. The snow layer is approximately 15 cm thick (except for over the nilas where there is only small amounts of snow), and covers major parts of the sea ice surface. The bright signatures of grey/white (1) ice is distinctly separable from the obviously more dark signatures of FY ice (2) (also note a different texture). The very dark signature of nilas, found in the polynya in area 3, is more difficult to separate from both calm open water, and level fast ice.

6 COMPARISON OF RADARSAT AND ERS-2 SEA ICE SIGNATURES

Within about only five hours on April 30, both RADARSAT ScanSAR and ERS-2 SAR data were acquired over the same area in the Kara Sea. Near simultaneous with the SAR image acquisitions, two icebreaker expeditions operated in the area, performing sea ice observations. This makes it possible to quantify similarities and differences of performance of the two sensors over sea ice environments. For this study, high-resolution RADARSAT ScanSAR and low-resolution ERS-2 data have been used, with an image pixel resolution of 100*100 for both sensors. Due to no calibration provided with the RADARSAT data, only relative comparisons are possible. Overall, the images from the two sensors look similar, and the same features and details are evident in both images. Some features have drifted during the five hour time displacement, for example the large/giant first-year ice floes around 74°N/77°E and 73°N/78°E, and the smaller floes in the upper part of the image (about 74°15N). The main drift direction is westwards. More detailed analysis of the two sensors has been performed, by comparing profiles along distinct ice features in the two images.

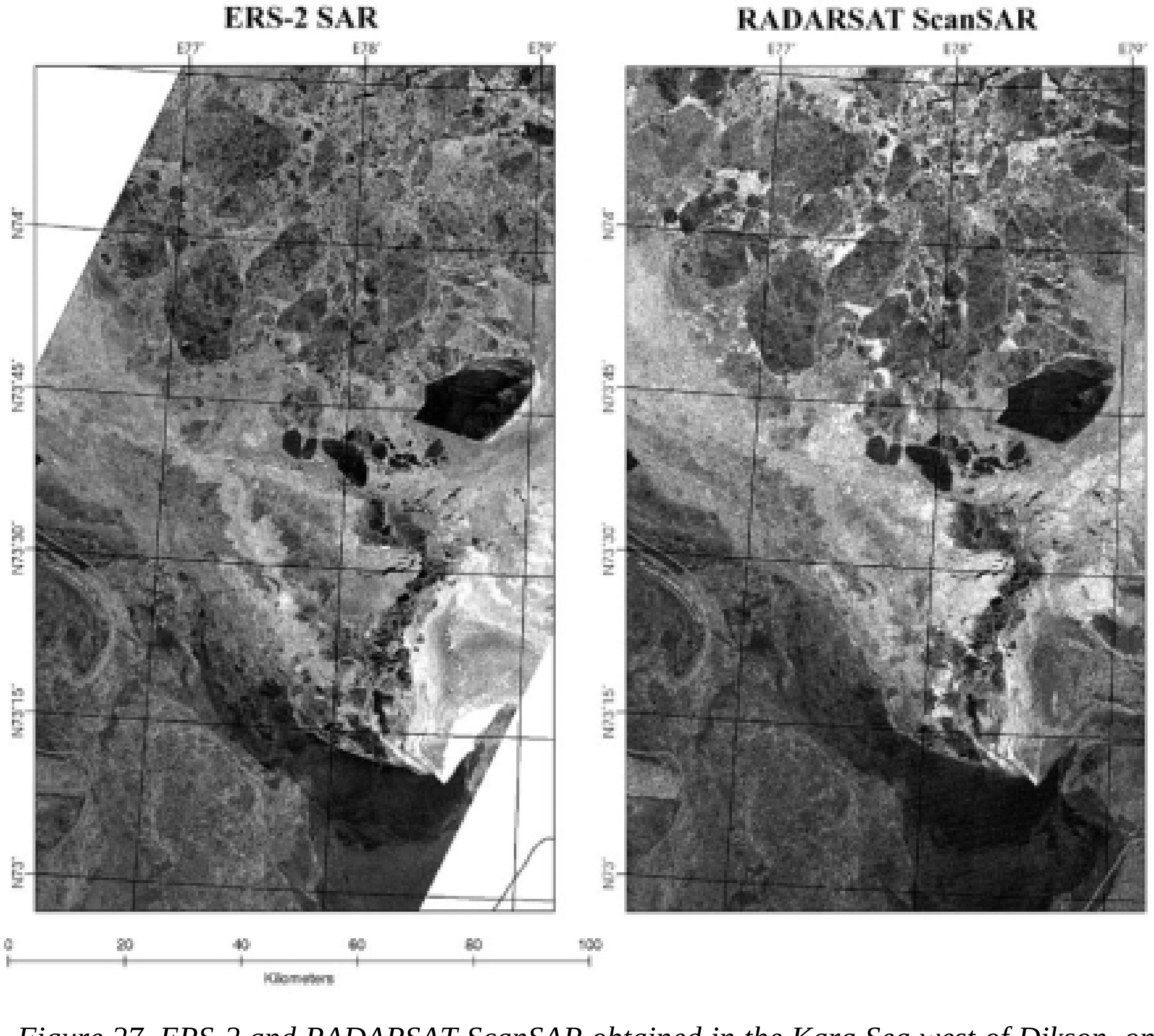

*Figure 27. ERS-2 and RADARSAT ScanSAR obtained in the Kara Sea west of Dikson, on April 30. The pixel resolution is 100*100m for both images. The lower part of the images was covered by level and hummocked fast ice. The drift ice just outside the fast ice zone consisted of a mixture of new/young ice and small first-year ice floes. Farther north the drift ice consists mainly of large and giant first-year ice floes interleaved smaller cracks and leads, covered by new and young ice.*

Figure 28. A mosaic of ERS-2 and RADARSAT showing the position of the discussed profiles.

6.1 PROFILE A: OPEN WATER/NEW ICE

The most obvious difference between the two sensors was found within areas consisting of open water and/or new ice, as can be seen from Figure 29. The average mean brightness value is 75 in the RADARSAT ScanSAR image and 210 in the ERS-2 image. Recent studies [Johannessen,. *et al*, 1999] have shown that there is a constant bias between the ERS-2 SAR and RADARSAT ScanSAR backscatter signals over open water and sea ice. This means that the image brightness differences observed for the two sensors are due to different polarisation and incidence angle. Using this knowledge it can be shown that the wind conditions were the same during the two SAR acquisitions. In this study the calibration equation giving radar backscatter values for RADARSAT ScanSAR images was determined using simultaneously ERS-2 SAR data.

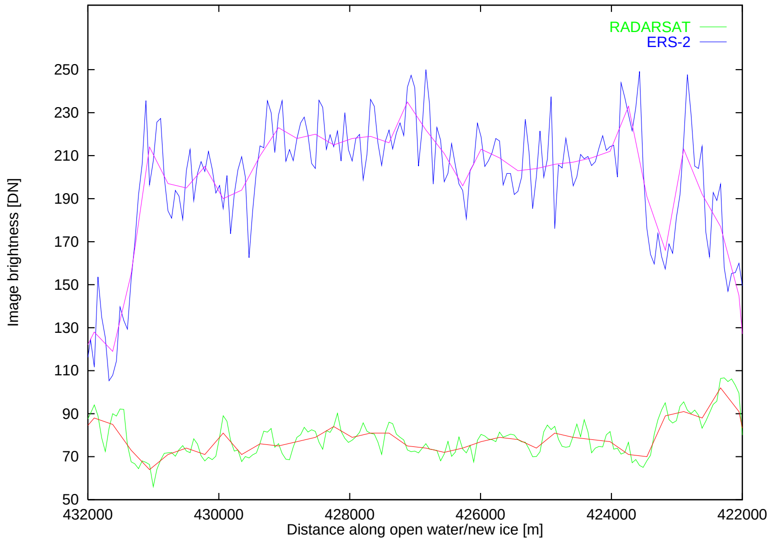

Figure 29. Open water/new ice

6.2 PROFILE B: LEVEL FAST ICE

Level fast ice is the darkest feature found in the images, and for this ice situation the two sensors observe very similar. Both have an average mean brightness value of 50, and a standard deviation of 5.

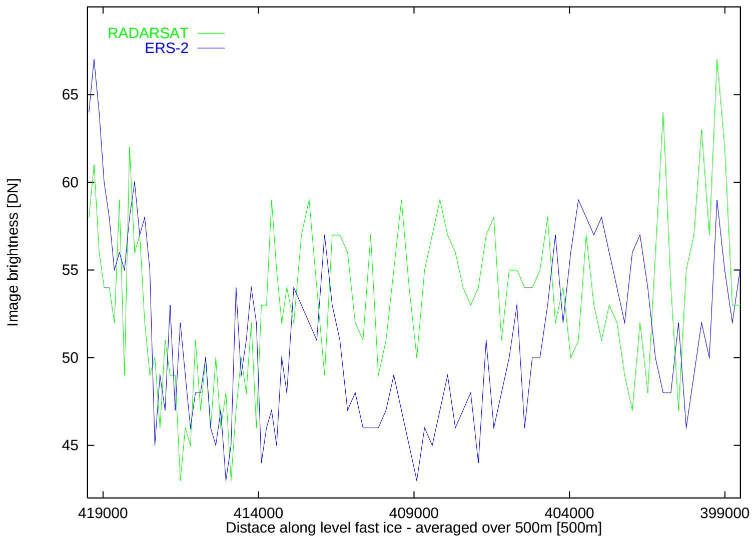

Figure 30. Level fast ice

6.3 PROFILE C: DEFORMED FIRST-YEAR ICE

Along this profile the individual floes are more distinct in the ERS-2 image than in the RADARSAT image, but the overall trend is similar.

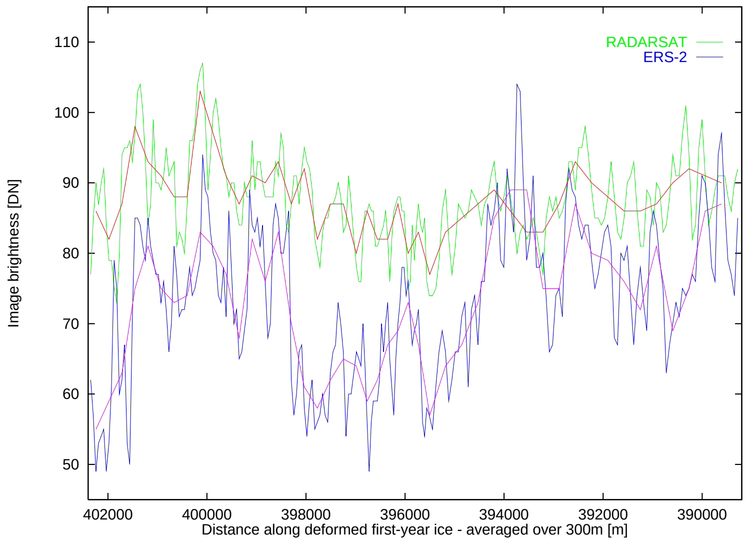

Figure 31. Deformed first-year ice.

6.4 PROFILE D: GIANT LEVEL FIRST-YEAR ICE FLOE

Along this profile the sensors observe similar. Due to ice drift, there is a horizontal off-set between the two profiles for the rapid increase in brightness at the end of the profile. Apparently, this ice floe is a former part of the Yenisei estuary fast ice zone.

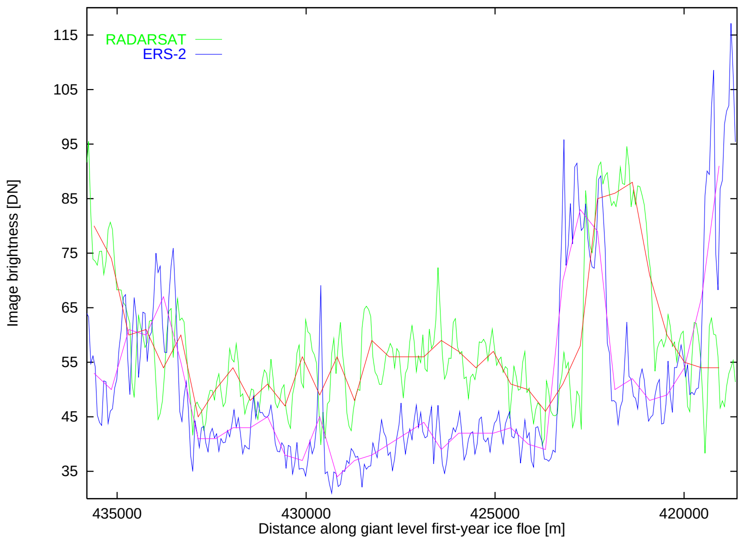

Figure 32. Giant level first-year ice floe

6.5 PROFILE E: SMALL FIRST-YEAR ICE FLOES AND NEW/YOUNG ICE

These profiles are more difficult to compare, because the ice drift between acquisitions. The average mean value of the two sensors are similar, around 80. The RADARSAT ScanSAR signals have a standard deviation of 22, and for ERS-2 this value is 14.

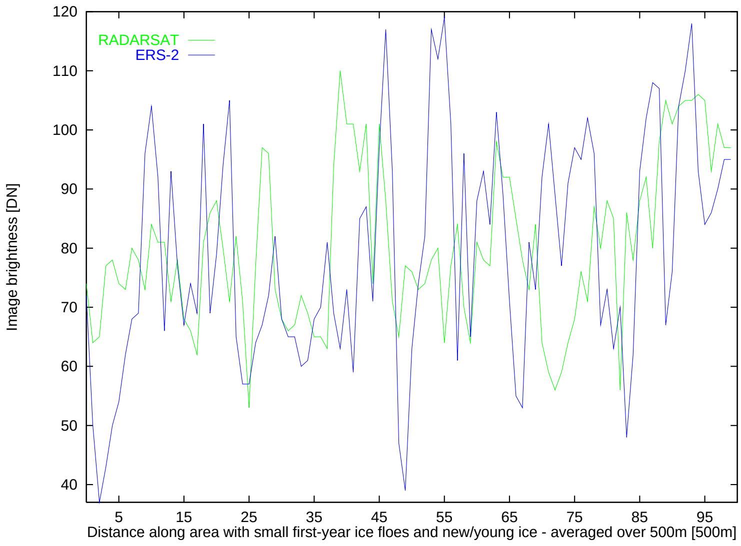

Figure 33. Small first-year ice floes and new/young ice

6.6 PROFILE F: YOUNG ICE

In this region the average mean of the RADARSAT signals are 100, distinct brighter than the mean value of 80 for the ERS-2 signals. The general trend of the profiles is similar, despite small horizontal displacements.

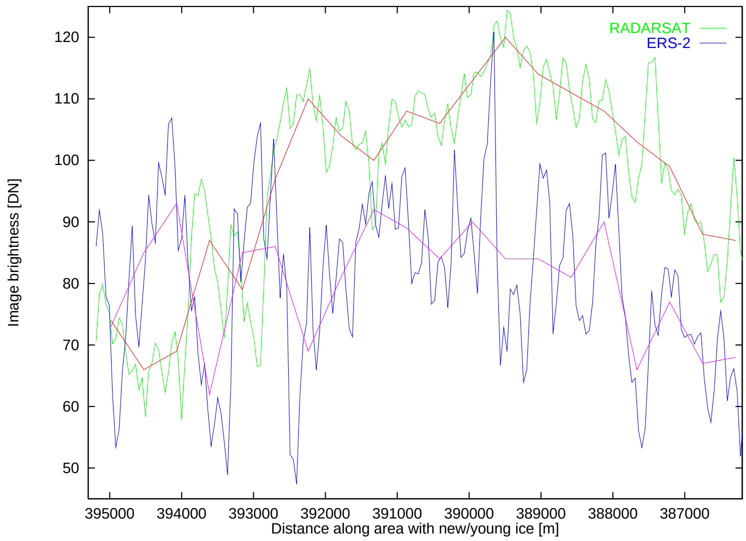

Figure 34. Young ice

7 COMPARISON OF RADARSAT SCANSAR AND SHIP PERFORMANCE

The ship position and corresponding performance (average speed and power use) have been compared on an hour-to-hour basis and superimposed on a SAR image obtained at about the same time the ARCDEV voyage passed through the imaged area. From Figure 35 it is possible to derive the SAR signature characteristics of different ship performances. The figure shows that during easy ice conditions the ship moved at a high and stable speed, using little power. During more difficult conditions the power consumption increased drastically while the ship speed was unstable and generally low.

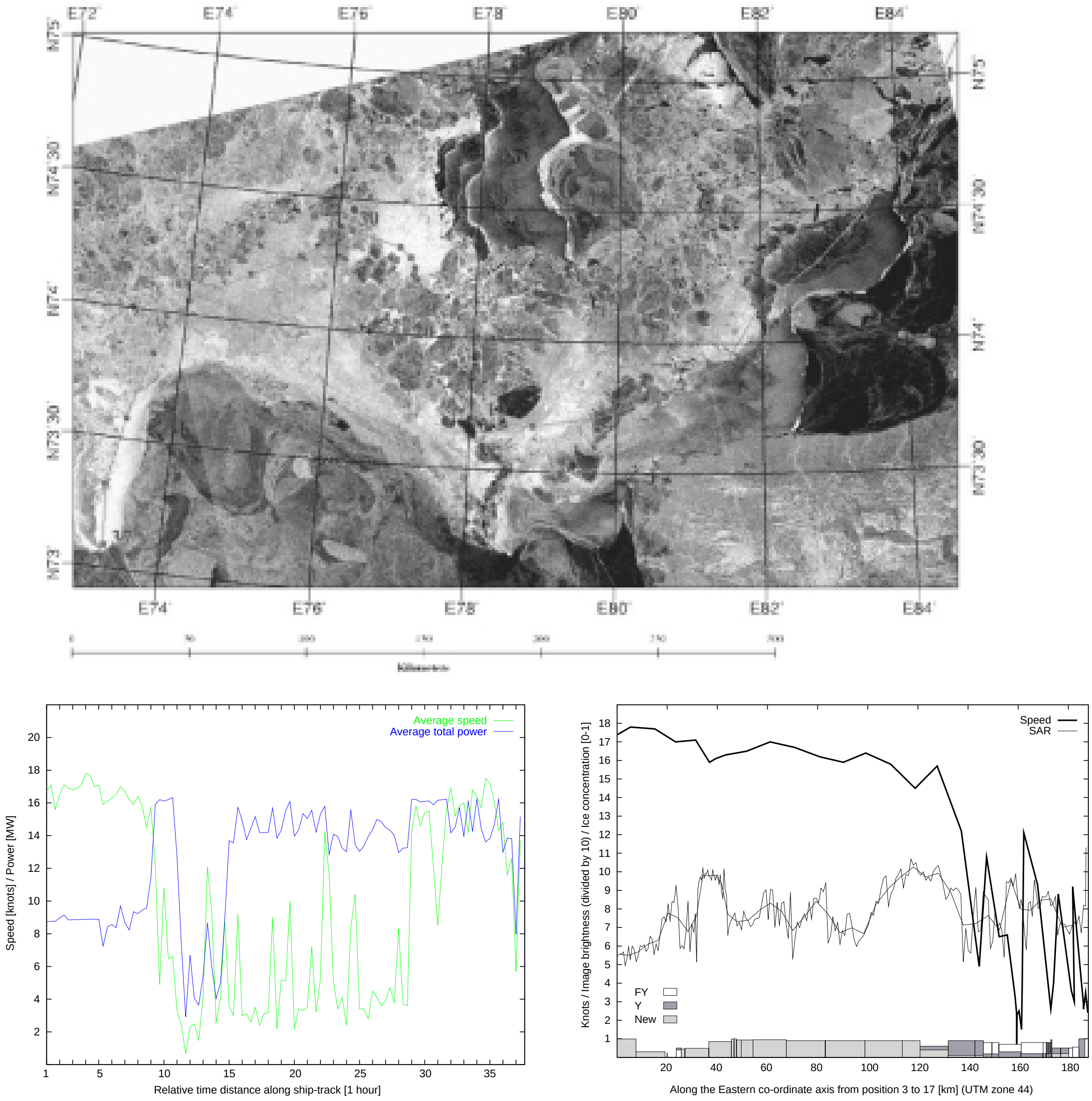

a) b) c)

Figure 35. a) Sub-image of RADARSAT ScanSAR of April 30. Superimposed in green is the ship track of i/b Kap. Dranitsyn from May 1 to 3. The distance between two red dots represent the distance travelled during 1 hour. b) The average speed and power consume of the ship on an hour-to-hour basis within the same time interval. c) Profile of the speed from point 3-17 with corresponding RADARSAT image brightness values and ice observations from the bridge.

Figure 35 c) is an enhancement of the part of the speed profile where the most drastic speed drop occurred, together with the corresponding RADARSAT SAR signatures and ice observations from the ship-bridge. Due to about one and a half day time separation between the SAR acquisition and ice observations from the ship the observed situations can be somewhat different. The first half of the profile is over new ice, and the ship speed is high and stable, despite a high ice concentration. The SAR signature values are typical for areas with thin ice like nilas and calm open water. At about 130km the ship speed drops drastically at the same time as the dominating ice feature changes to young ice (up to 30cm thick). From hereon the ship speed varies significantly and the ice condition is dominated by young ice and firstyear ice (up to 120cm thick). The average SAR signature value is higher, which indicates young ice and ridged firstyear ice. The darkest signals correspond to more level firstyear ice, and are similar to the values observed for new ice. Different texture makes these two ice types separable. At about 40km there is a distinct increase in the SAR signature not reflected in the speed profile, presumably this ice feature had moved before the ship entered the area.

Figure 35 clearly demonstrates the need for, and usefulness of high-quality sea ice information as support for both regional and tactical navigation tasks. In this manner RADARSAT ScanSAR data are efficient tools for supporting the efficiency of ship navigation in ice covered waters.

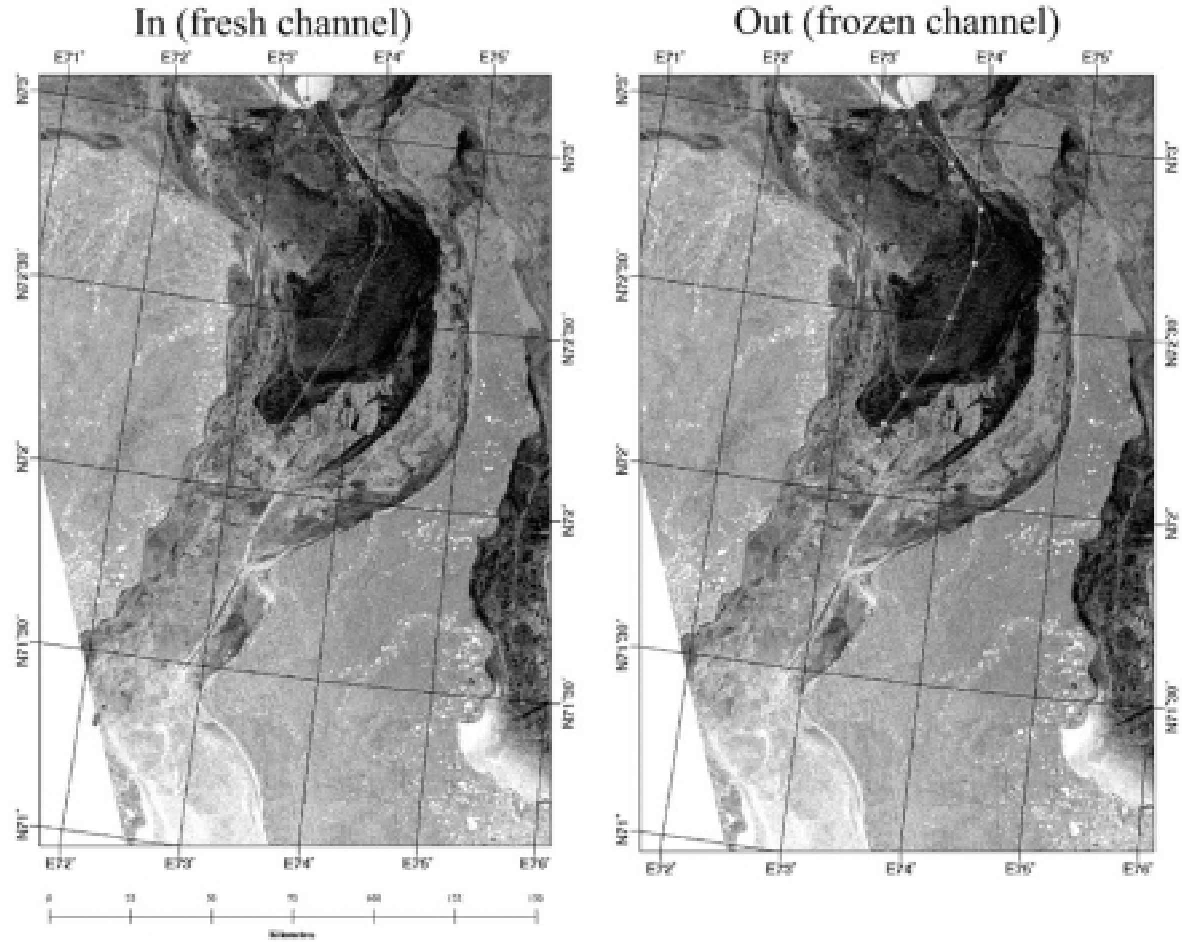

Figure 36. Speed of convoy in and out of Ob estuary. There is one hour between each dot in the two images. The prepared ice channel was frozen, and at certain parts closed, before the return voyage. As it appears, i/b Kapitan Dranitsyn had to struggle to get through the most ridged part of the fast ice (up to 72°10N).

The hourly position of the convoy on its way in and out of the Ob estuary is plotted on the ERS-2 image of May 6. As can be seen in Figure 36, the convoy proceeded fast and steady in the estuary when prepared channel in the fast ice was fresh. Before the returning voyage 5 days later, parts of the channel had closed, and i/b Kapitan Dranitsyn had difficulties crossing the ridged fast ice area up to about 72°10N (seen as quite bright in the image). In the level fast ice zone farther north, the speed in and out was similar. This figure demonstrates how important the ERS-2 SAR image of April 17 was for the planning and preparation of the fast ice channel. As the ice surface was fully covered by snow at this period, it is necessarily to use SAR data for planning of this kind of operations, utilising the sensor's ability to penetrate dry snow.

8 AUTOMATIC CLASSIFICATION PROCEDURES

Manual image analysis and ice classification by expert personnel provides high quality sea ice maps, but is time consuming. Ideally, automatic classification algorithms can meet the user requirements for classification quality (level of detail and image resolution) and processing time. We have trained and assessed the performance of two automatic sea ice classification algorithms, one based on Linear Discriminate Analysis (LDA) and one on Back-propagation Neural Network (BNN).

8.1 DESCRIPTION OF THE ALGORITHMS

The tested algorithms use both local statistical measures and texture parameters of the radar image. Use of texture features in addition to the mean radar backscatter value can improve the classification accuracy [Shokr 1991, Barber *et al.* 1993]. Standard texture parameters based on Grey Level Co-occurrence Matrix (GLCM) are used [Haralick *et al. 1973*]. The texture measures include contrast, cluster shade, cluster prominence, inverse difference moment, homogeneity and entropy. Local statistical parameters have been found useful for automatic classification, and superior to texture parameters for separation of sea ice types [Wackerman and Miller, 1996, Nystuen and Garcia, 1992]. In addition to the texture measures and mean brightness value, we used second, third and fourth order statistical moments. All features were computed over 9 by 9 pixels. This window is large enough to describe the texture and provide the necessary inputs to the GLCM, and still small enough to avoid a mixture of too many different sea ice types.

The first algorithm, by Wackerman and Miller [1996], uses a conventional statistical classification approach based on Linear Discriminate Analysis (LDA algorithm). In addition to mean grey level intensity, this algorithm uses 15 different texture and statistical measures for separating the ice classes. It is assumed that the probability distribution for each class is a multivariate normal. All pixels in a window are classified as class *a* if its feature vector falls inside the feature space region corresponding to class *a*. The position of the decision boundaries is determined during the training procedure, seeking maximum separation of the different sea ice classes [Wackerman and Miller, 1992]. As the classification window moves around in the image each pixel is classified a number of times, and finally assigned to the class it is most frequently classified as.

The second approach uses a fully connected multi-layer, feed-forward back-propagation Neural Network - BNN algorithm [Bishop, 1995]. The information propagates in one direction from the input processing units to the output processing units. The input to a processing unit is a weighted sum of the outputs from the previous layer. During an iterative training procedure the weights between the processing units are adjusted. The well-known distribution free back-propagation method was used for the training. During the training procedure complex forms of decision boundaries can be constructed. This advantage is especially valuable if in the feature space the different class clusters complex forms and is interlocked. We tested various numbers of hidden layers and proceeding units for the Neural Networks, and a combination with 16 input-nodes (texture and statistical measures), 70 nodes in the first layer and 50 in the second, and 6 output-nodes (different ice classes) was selected.

8.2 TRAINING AND VALIDATION

The RADARSAT Scan SAR images of April 25 May 8, 1998 were used for selecting the training data. The training data was grouped into 9 ice classes:
1) Level firstyear ice, 2) Deformed firstyear ice, 3) Very deformed first year ice, 4) Young ice, 5) New ice, 6) Open water and nilas, 7) Level fast ice, 8) Deformed fast ice, and 9) River ice. Muliyear ice was not found in any of 6 RADARSAT scenes acquired for the expedition. Only four squares with a size of 30 by 30 pixels were available for the *Open water and nilas* class, which is a bit too low to fully capture its distribution in the feature space. The boundary between drifting and fast ice was manually determined using bathimetry data, *in situ* observations and successive SAR images. These areas was classified separately, in order to avoid errors caused by misclassification of level fast ice as open water, as these classes have poor texture and nearly similar brightness' in SAR images. Homogeneous regions containing the chosen sea ice classes were used for training, while the whole image was used for the classification.

8.3 RESULTS

All obtained RADARSAT ScanSAR images were classified. The performance of the two algorithms have been assessed by comparing the classification results of the images of April 30 and May 8.

The RADARSAT ScanSAR image of April 30 is a fully independent image concerning drift ice, while training regions for fast ice and river ice were collected here. Both algorithms classified most of the young ice correctly, while they miss-classified the deformed first year ice north of Belyi island. Overall, the LDA algorithm performed better. See Figure 37.

On the image of May 8 the classification by the BNN algorithm was superior to the results of the LDA algorithm for most ice classes. Fast and river ice is classified by the LDA algorithm in both cases. The Training regions for New ice, Level and Very deformed first year ice were taken from this image, and as such this is not a fully independent image. Nevertheless it is still interesting to see location of the border between different sea ice types, as only rectangular regions were used for the training. Very deformed firstyear ice at the Kara Gate region, and Deformed first year ice along the Eastern Coast of Novaya Zemlya and along the Yamal Coast is better classified by BNN algorithm. Also separate firstyear ice ridges ice are better delineated by this algorithm. As expected, the BNN algorithm is more sensitive to the lack of enough proper training data. For example was the flaw polynya along the Yamal Coast miss-classified as level first year ice by BNN algorithm, while the LDA algorithm classified parts of it correctly.

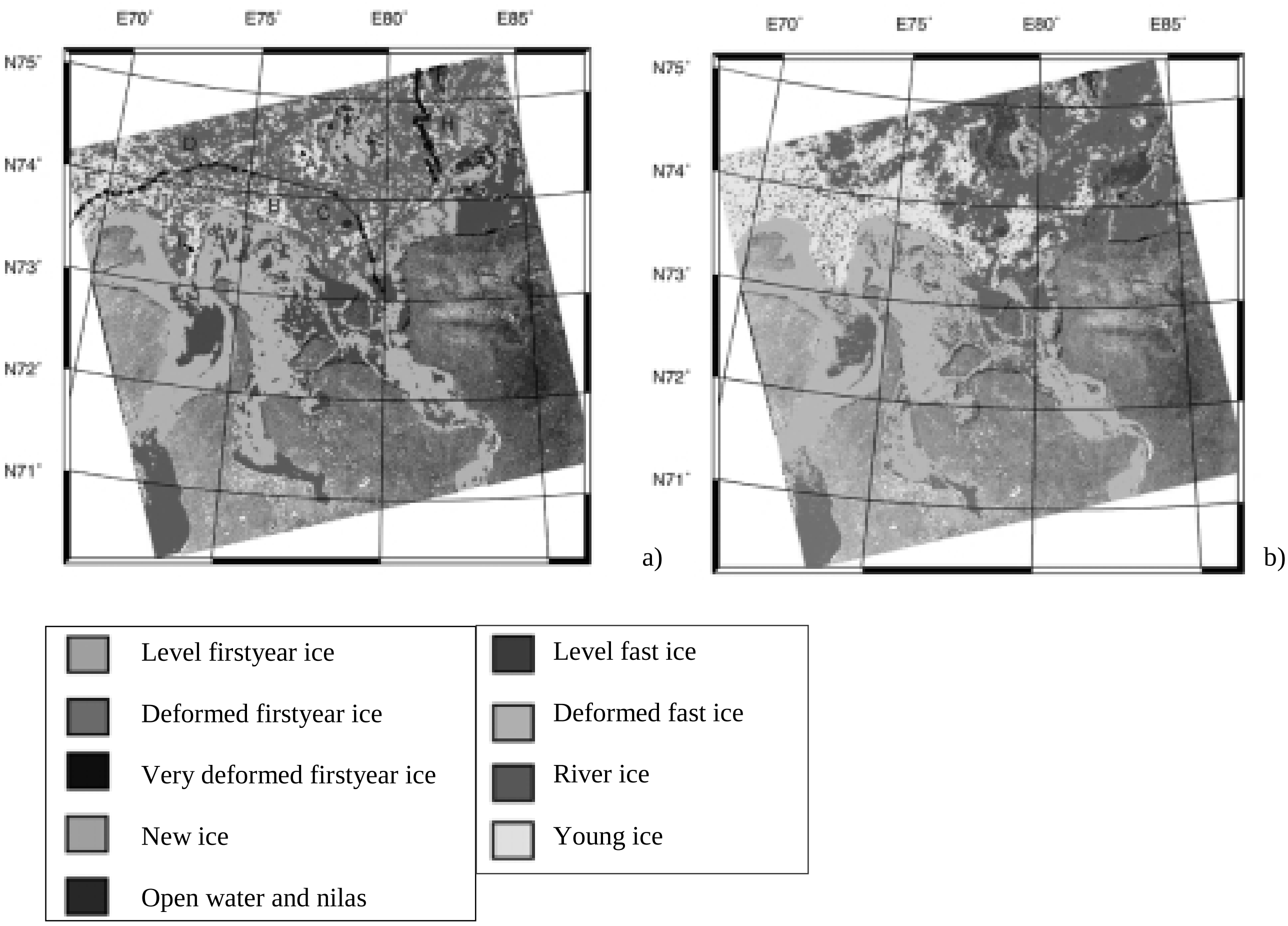

Figure 37. Classification results for the RADARSAT ScanSAR image of April 30, using a) Linear Discriminate Analysis (LDA) and b) Back-propagation Neural Network (BNN).

9 DISCUSSION AND CONCLUSION

Results of the thematic interpretation of the sea ice information in the ERS and RADARSAT SAR images demonstrate the practical use for Arctic ice navigation. The RADARSAT ScanSAR images of April 23 are a valid example of practical use of satellite SAR data for strategic planning of ice navigation operations. From these images the northern routing alternative to the Kara Gate was selected. As an example of use of satellite SAR data in tactical navigation planning, the image of April 30 was used for selecting the optimal steering along the shores of Taymyr and Yenisei to the Ob estuary from the east. Despite a longer physical travelling distance, in a region with very difficult ice conditions, about 65% of the route consisted of either new or young ice, i.e. very easy ice conditions. The main advantages of satellite SAR data compared to the traditional optical satellite data was demonstrated within the very difficult ice navigation conditions in the fast ice in the Ob estuary. From two ERS-2 SAR scenes of April 17, the most efficient route along easier ice conditions, could be identified. Analysis of SAR and *in situ* data from the estuary after the preparation of the ice channel clearly demonstrate how the icebreaker moved along more level ice, avoiding hummocks and ridges. As a result, the first ever winter icebreaking operation in the Ob estuary became a success.

Characteristic RADARSAT ScanSAR signatures of different ice types have been retrieved on the basis of sub-satellite visual ice observation and classification, photographs, and joint analysis with ERS SAR data. Comparison of RADARSAT ScanSAR data with *in situ* observations resolves that the radar backscatter signatures of different ice types are not unique, as for instance young ice and deformed first-year ice. Therefore, both texture and contextual information is important in order to perform ice type classifications based on the brightness signatures in a radar image. The classical approach for visual interpretation of satellite images also includes use of auxiliary information, such as hydrometeorological observations, ice drift data, previous observations by other remote sensing sensors, and knowledge and experience of the general ice situation for various seasons in the region. Location, time and surrounding ice conditions are useful for the image interpretation. Logical features limit the appearance of some ice types in different seasons and in different regions of the Arctic Seas. River ice can be distinguished using logical features, and the fast ice boundaries from analysis of successive images.

The RADARSAT signatures of new and young ice will vary considerably, depending on the ice type and state of the surface. Nilas is seen as homogenous areas with dark backscatter values, while grey ice have a very high signal, and is clearly distinguishable from nilas. The brightness of grey/white ice varies from dark to rather light, depending on thickness and surface deformation. First-year ice will vary from dark to light, mainly depending on the degree of ridging. Level ice give a very dark backscatter signal, while heavy ridged and deformed first-year ice can be as bright as grey ice. Although the image brightness values of first-year ice and grey or grey/white ice tend to be similar, they can be separated due to differences in the texture. Level land-fast first-year ice has a very dark signature value, very similar to calm open water. Contextual information, such as position and time of the year, is often necessarily in order to separate these two situations. Leads and fractures, both unfrozen or covered with new or young ice, can be identified in RADARSAT images. This is very important for selecting an optimal navigation route in the ice.

ERS-2 and RADARSAT ScanSAR data have proved to be an efficient tool for ice navigation support of ARCDEV and other convoys in the Russian Arctic. Nevertheless, the thematic decoding is still fragile, in particular the usage of automatic decoding procedures. In order to create robust classification of different ice phenomenon, more research is needed on data processing and image calibration, texture measures, and use of auxiliary information. Means for reducing the image file size, while still preserving the vital information is also important, together with more cost-efficient methods for data communication for transmission, and use of the information onboard the icebreakers.

Data on typical convoy speed in different ice conditions are presented in the following table:

Ice conditions	Convoy speed
Polynya (open water, nilas, grey, grey-white, pancake ice)	11 – 14 knots
Areas with mixture of first-year ice with new and young ice	6 – 13 knots
Thin first-year ice	10 - 11 knots
Level thick and medium first-year ice	2 – 10 knots, stuck in ice
Ridged first-year ice	2 – 5 knots, stuck in ice
Level fast ice (ice thickness 130 – 150 cm)	7 – 8 knots

Analysis of these data shows that selection of optimal routes through lighter ice conditions will increase the average convoy speed significantly. Add to this the safety aspects of the ice operation, and that if the convoy gets stuck in the ice, much time is lost towing the ships to more easy conditions. It was estimated by MOH during the expedition, that use of RADARSAT ScanSAR data for navigation support in the drift ice, can increase the overall ship speed by a factor of at least two.

ACKNOWLEDGEMENT

RADARSAT ScanSAR data were provided and purchased by the Canadian Space Agency (CSA) under ADRO project no. 289.

ERS-2 SAR data were purchased from the European Space Agency (ESA) by the ICE ROUTES project funded by the European Commission Transport RTD Programme (Contract no. WA-96-AM-1136).

All near-real time data were made available from Tromsø Satellite Station in Norway.

PUBLICATIONS:

Results from this work have been published at the following proceedings:

Pettersson, L.H., Sandven, S., Dalen, Ø., Melentyev, V., Babich, N.I., 1999. Satellite radar ice monitoring for ice navigation of the ARCDEV tanker convoy in the Kara Sea, The 15th International Conference on Port and Ocean Engineering under Arctic Conditions (POAC), Helsinki, Aug. 23-17, 1999.

Pettersson, L.H., Sandven, S., Dalen, Ø., Melentyev, V., Babich, N.I., 1999. Satellite radar ice monitoring for ice navigation of a tanker convoy in the Kara Sea, IGARSS'99, Hamburg Jun. 28-Jul 02, 1999.

REFERENCES:

Barber, D.G, Shokr, M.E., Fernandes, R.A., Soulis, E.D., Flett, D.G., and LeDrew, E.F., 1993, A comparison of second-order classifiers for SAR sea ice discrimination, Photogrammetric Eng. and Remote Sens, 59, 1397-1408.

Bishop, C.M, 1995, Neural networks for pattern recognition, Clarendon Press, Oxford, 481p.

Haralick, R.M., Shanmugam, K., and Dinstein, I., 1973, Textural features for image classification, IEEE Trans. Systems, Man Cyber., SMC-3, 610-621.

Johannessen, O. M., A. M. Volkov, V. D. Grischenko, L. P. Bobylev, S. Sandven, K. Kloster, T. Hamre, V. Asmus, V. G. Smirnov, V. V. Melentyev and L. Zaitsev, 1998, ICEWATCH - Ice SAR monitoring of the Northern Sea Route. In "Operational Oceanography. The Challenge for European Co-operation" (Editor in Chief: J. H. Stel). Proceeedings of the First International Conference on EuroGOOS, 7 -11 October 1996, The Hague, The Netherlands. Elsevier Oceanography Series, No. 62, 1997b, pp. 224 - 233.

Johannessen, .O. M., A. M. Volkov, V. D. Grischenko, L. P. Bobylev, S. Sandven, K. Kloster, T. Hamre, V. Asmus, V. G. Smirnov, V. V. Melentyev and L. Zaitsev, 1999, ICEWATCH: Demonstration of satellite SAR data in ice navigation in the Northen Sea Route, The 15th International Conference on Port and Ocean Engineering under Arctic Conditions (POAC), Helsinki, Aug. 23-17, 1999.

Johannssen, O.M, Alexandrov, V.Y., Sandven, S., Pettersson, L.H, Bobylev, L.P., Khizhnichenko, V.M., Volkov, A.M., Lundhaug, M., Dalen, Ø., Kloster, K., Bogdanov, A.V., and Zaitsev, L.V., 1999, Synergistic use of RADARSAT, ERS and Okean radar images for Sea Ice Studies in the Northern Sea Route, IGARSS'99.

Nystuen, J.N., and Garcia, F.W., 1992, Sea ice classification using SAR backscatter statistics, IEEE Trans. On Geosc. and Remote Sensing, 30, 502-509.

Sohkr, M.E., 1991, Evaluation of second-order texture parameters for sea ice classification from radar images, J. Geophys. Res., 96, 11-13.

Wackerman, C. and Miller, D., 1996, An automated algorithm for sea ice classification in the Marginal Ice Zone using ERS-1 Synthetic Aperture Radar, ERIM Technical report no. 252000-25-T.